DATA-DRIVEN MULTI-SCALE HOMOGENIZATION FOR COMPOSITE MATERIALS

by

EZE CHUKWUEMEKA CHARLES
(220112357)

Submitted in fulfillment of the requirements for the degree of
Master of Science in Civil Engineering

College of Agriculture, Engineering and Science
University of KwaZulu-Natal
Durban

2nd December 2021

SUPERVISOR:
Dr Georgios A. Drosopoulos

DECLARATION OF PLAGIARISM

I, Eze Chukwuemeka Charles, declare that:

1. The research reported in this thesis, except where otherwise indicated, is my original research.

2. This research has not been submitted for any degree or examination at any other university.

3. This thesis does not contain other persons' data, pictures, graphs, or other information unless specifically acknowledged as being sourced from other persons.

4. This research does not contain other persons' writing unless specifically acknowledged as being sourced from other researchers. Where other written sources have been quoted, then:

    a. Their words have been re-written but the general information attributed to them has been referenced.

    b. Where their exact words have been used, then their writing has been placed in italics and inside quotation marks and referenced.

5. This thesis does not contain text, graphics or tables copied and pasted from the Internet, unless specifically acknowledged, and the source is detailed in the thesis and the References sections.

Signed/ Date

[redacted] 2/12/2021

……………………………

Eze Chukwuemeka Charles

PREFACE

The research which is presented in this thesis was performed through the school of Engineering, Civil Engineering department of the University of KwaZulu-Natal, Durban, from March 2021 to December 2021, under the supervision of Dr. Georgios A. Drosopoulos.

As the Candidate's Supervisor, I agree to the submission of this thesis.

……………………………….. signed at … Preston, UK …… on ……1/12/2021………..

DEDICATION

This world is dedicated to Almighty God for his Grace and Guidance upon my life and to my dear parents, Mr. and Mrs. Eze Anthony Chukwuemeka, Words cannot express my profound gratitude for all that you have done and continue to do for me. Thank you.

ACKNOWLEDGMENT

I would like to express my sincere gratitude, thanks, and appreciation to my supervisor, Dr. Georgios Drosopoulos, for his time, guidance, support, and encouragement that has facilitated the successful completion of this research. Thank you for the knowledge you have imparted to me, your willingness in assisting my endeavors, and your instrumental supervision throughout this year.

I would also like to show my appreciation to:

- Bar. & Dr (Mrs.) Emmanuel Ugwu for their support, morally and financially throughout this research. Thank you so much for your efforts in my life, I appreciate it.
- My parents, Mr & Mrs. Eze Anthony C, and my siblings for their constant support morally, financially, and spiritually. God bless you so much.
- My extended family, relatives, and friends thank you so much for your constant support. God bless you all.

LIST OF FIGURES

TABLE OF CONTENT

CHAPTER ONE

INTRODUCTION AND BACKGROUND

Material is the building block of any structure. The structure might be natural (for example timber or bone) or man-made (for example wall). In engineering and material science, any material which is studied, basically because of its mechanical properties is called a structural material (Vasiliev & Morozov, Mechanics and Analysis of Composite Materials, 2001). The main two mechanical properties or characteristics of structural material are its strength and stiffness because it helps it to maintain its shape when acted upon by forces. (Vasiliev & Morozov, Mechanics and Analysis of Composite Materials, 2001).

From time immemorial, different materials have been joined to produce stronger and enhanced materials. This dates back to the era of the clay and stone age. When clay is used for construction, it is strengthened with struts to create a stronger wall. This enhanced wall is a composite. Other composites used then are, chariots, bone, horns, etc (Blessley, 2002). Another common composite is concrete, gotten by the combination of cement, water, and aggregates. Reinforced concrete is another composite material with improved properties which is gotten by combing concrete and metal.

A composite material consists of two or more components with unlike properties. The composite formed has improved properties, and these properties are better than the properties of the individual components. According to Dhakal and Ismail, (Dhakal & Ismail, 2021), a composite is made up of two or more materials with different properties which produce a material(composite) with better properties, and still retain their individual properties. Therefore, when two or more dissimilar materials are joined, such that they are separated by an interface, to form a new material with an improved property, a composite material is formed.

Despite being available for several years, composite materials have been a wonderful and active research topic in engineering and material science (Balokas, Czichon, & Rolfes, 2018). It has also been used in design in engineering (Wriggers, Zavarise, & Zohdi, 1998). The manner a complex structure behaves is a function of the nature of the constituents that makes up the structure (Drosopoulos & Stavroulakis, Data-driven Computational Homogenization Using Neural Networks:FE2-NN Application on Damaged Masonry, 2020).

To design or analyze a composite material usually requires a numerical method. This is because the analysis of a composite usually involves complex geometries, loadings, and material properties. Finite Element Method (FEM) or Finite Element Analysis (FEA) is a numerical method that helps in the analysis and design of the composite structure.

FEM is a method for finding the numerical solution of a partial differential equation by translating it into an algebraic equation that can be solved (Seshu, 2003). In engineering, FEM can also be referred to as a computational technique that provides approximate solutions to boundary value issues (Hutton, 2004). According to Nikishkov, (Nikishkov, 2004) FEM is a numerical methodology for addressing problems involving partial differential equations or functional optimization.

A lot of engineering and scientific problems take the form of multiple scales. Multi-scale in the sense that it involves different scales or levels of analysis. Multiscale analysis of a composite involves the analysis of the composite in two scales namely, the microstructural scale and the macrostructural scale. Multiscale simulation has its application in so many fields such as mathematics, computer science, material science, etc. It is proposed to solve for the effective and accurate behaviour of a composite whose constituents have an imperfect interface (Shu & Stanciulescu, 2020). When nonlinearities are present, modern multiscale methods are based on sophisticated state-of-the-art computational tools (Geers M. G., Kouznetsova, Matouš, &

Yvonnet, 2017). To analyze a composite material is always difficult as its constituents may experience a lot of multiscale fluctuations in elasticity behaviour, electrical or thermal behaviour, conductivity behaviour, and so on (Efendiev & Hou, 2009).

Homogenization is the process of considering a Representative Volume Element (RVE), which is a statistically homogeneous representation of the composite material, used to estimate the stresses and strains in the matrix and fibres (Voyiadjis & Kattan, 2005). Also, the homogenization methodology can be defined as an iterative applied mathematics method that produces an approximate effective equation for material response at macroscopic length scales under specified technical assumptions (Arbabi, Bunder , Samaey, Roberts, & Kervrekidis, 2020). Homogenization of a composite structure aims at considering the behaviour of the microscopic model while solving for the behaviour of a macroscopic structure.

Traditional computational homogenization is always faced with a lot of challenges in which expensive computational time and memory is the major challenge. But these challenges can be solved with the use of machine learning and data-driven technique.

"Data" refers to any knowledge that aids in the definition of a mathematical issue, regardless of whether it originates from an experiment. We use the phrase "material data" to refer to any information that aids in the definition of material behaviour, regardless of whether it comes from an experiment. Multiscale analysis, first-principles computations, and other methods, for example, can be used to obtain material data of the type of data-driven (Conti, Müller, & Ortiz, 2018).

By formulating the problem directly on a given material data set while enforcing relevant restrictions and conservation rules, the Data-Driven methodology for computational mechanics avoids any modeling stage. This technique, in particular, leads to a distance optimization problem between a given material data set and the subset of field pairs that fulfill the conservation laws by establishing a phase space of stress-strain field pairs (Karapiperis, Stainier, Ortiz, & Andrade, 2021).

Artificial Neural Networks (ANN) can be used as an alternative. ANN has gotten a lot of attention recently, especially in the context of deep learning, owing to its influence on areas like computer vision, speech recognition, and automated vehicles (Henkes, Caylak, & Mahnken, 2021).

The node features, learning rules, and network topology all contribute to the definition of a neural network. The learning rules ensure that the network's performance is improved by making appropriate adaptive modifications to the link weights. Furthermore, due to the increased number of locally connected nodes, one of the most striking aspects of neural networks is their high failure tolerance (Stavroulakis, Avdelas, Abdalla, & Panagiotopoulos, 1997).

A multilayer feedforward neural network can be trained to recognize and interpret experimental data using the error-correcting back-propagation algorithm (Stavroulakis, Avdelas, Abdalla, & Panagiotopoulos, 1997).

This research aims to use data-driven multiscale homogenization to simulate and get the effective behaviour of a fibre-reinforced composite material. That is to use databases (data-driven), substituting the stress-strain laws, in finite element analysis of composite materials.

In this dissertation, a data-driven computational homogenization technique is utilized to solve for the effective behaviour and properties of a composite material.

Firstly, the RVE is analyzed using a particular loading strain. The stress and stiffness of the RVE were calculated at every integration or gauss point after the simulation. The integration or gauss point is the point within an element in which numerical integration is evaluated. The calculated stress and stiffness led to the generation of two databases; strain-stress database and strain-stiffness database which was used for the data-driven technique.

The two databases were trained using ANN. These trained databases were called at every integration point of the composite to calculate the stress and stiffness on the whole structure which is its effective properties.

Integration point is the point within an element at which integrals are evaluated numerically. It can also be called the gauss point. These points are determined in such a way that the numerical integration scheme's outputs are as accurate as possible. FEM software must employ numerical integration over the element volume at the gauss point, to obtain the stiffness matrix, as well as components of additional matrices.

1.1 AIM

This research aims to use data-driven multiscale homogenization to simulate and get the effective behaviour of a fibre-reinforced composite material. That is to use databases (data-driven), substituting the stress-strain laws, in finite element analysis of composite materials

1.2 OBJECTIVES

The objectives which form the crux of this research are:

- Graphical comparison of the results of the Neural Network (NN) predicted stress (Output) and the database base stress (target) in X, Y, and X-Y directions were obtained. The NN predicted stress is the output of the neural network which was calculated after training the neural network. X, Y, and X-Y directions are the directions in which the composite is being loaded, using the loading strain in the same direction.
- A graphical comparison of the output and target stiffness was obtained
- The force-displacement relationship was determined

- The effect of mesh size on the force-displacement relationship was determined
- The rate of debonding between different macro elements was determined.
- A plot of macro deformation of the composite structure was determined.
- The effect of change in load direction on the force-displacement relationship was determined
- Comparison between the traditional multiscale method to data-driven method on the force-displacement relationship when the direction of the macro load is changed from single downward loading to combined loading (loading from top, bottom, and right side of the composite)

1.3 ARRANGEMENT OF THE DISSERTATION

This dissertation consists of four chapters and is structured to provide a progressive and comprehensive understanding of the research undertaken in the study. The contents of each chapter are further elaborated on:

Chapter One: Chapter one introduces the concept of a composite material. It also contains the aims, objectives, and arrangement of the dissertation.

Chapter Two: This gives in detail all about composite structures and different pieces of literature review related to composites. It also discusses the different ways of simulating and obtaining the effective properties of the composite material.

Chapter Three: This chapter discusses the methodology adopted to achieve the aims and objectives of the research thesis.

Chapter Four: Presents the results and conclusion which gives the extent to which the aims and objectives were achieved.

CHAPTER TWO

LITERATURE REVIEW

Composite material is a heterogeneous material that is made up of two or more constituents. In most cases, these constituents are matrices that are normally reinforced with fibres.

2.1 PROPERTIES OF COMPOSITES

The main aim of using composite material in engineering is because it has an enhanced strength-to-weight ratio which reduces the overall weight of the components (Dhakal & Ismail, 2021). Other factors which drive the application of composite structures as stated by (Barberto, 2011) & (Oller S. , Numerical Simulation of Mechanical Behavior of Composite Materials, 2014) are;

- Composites have very high corrosion resistance.
- Composites are used where friction is usually experienced because they have high wear resistance.
- Composites, especially ones from ceramics have a low thermal expansion,
- Composites possess low or high thermal conductivity depending on where they are applied.
- Composites have enhanced fatigue life when compared to metals and alloys as they can withstand harsh conditions.
- They possess high mechanical strength at low density when compared to metals.
- Composites possess high resistance to various chemical agents
- Some composites are well resistant to moisture
- Most composite retains their properties when exposed to fire and elevated temperature.

2.2 CONSTITUENTS OF A COMPOSITE

A composite is normally made up of a matrix and a reinforcement element called fibres (Otero, Oller, Martinez, & Salomón, 2015), and the surface, bounding the fibre and the matrix is called a fibre-matrix interface (Bahl, 2021). The effective behaviour of a composite is greatly a function of the properties of the matrix and the reinforcements involved, and the bonding between them at the interface.

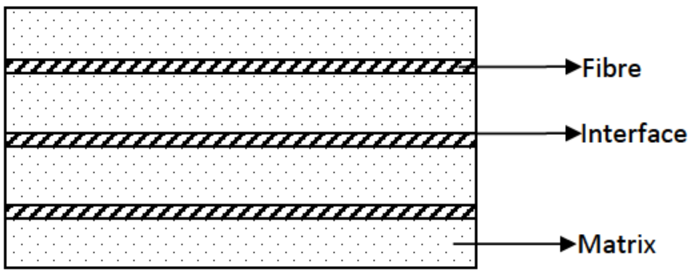

Figure 2.1: A Typical 2-D Representation of a Composite Material *Source:* (Herakovich, Mechanics of Fibrous Composites, 1998)

Matrix

Matrix is usually a continuous, isotropic, uniformly rigid material in a composite, in which reinforcements are immersed or embedded. It acts as a layer of protection for the reinforcements embedded in it and adds to the stability of the composites. The matrix should be uniformly distributed in a composite to avoid cracking where there is much of the matrix and voids where it is insufficient. The major role of a matrix is the transfer of loads to the reinforcements. It also helps to control cracking in composites. It is very weak when acted upon by a tensile load.

Function of Matrix

The importance of a matrix cannot be overemphasized in a composite as it performs the following functions (Blessley, 2002):

- It serves as a binding material for reinforcements in a composite material
- It helps in preserving the reinforcements by protecting them from harmful environmental effects
- It distributes loads on the composite uniformly to the reinforcements
- It helps to withstand cracks in composites
- It carries interlaminar shear and increases the transverse properties of a laminate
- It helps the composite to withstand impact and fracture
- It gives the composite its shape and encloses the reinforcements

Reinforcements

Any high-strength material which is integrated or embedded into the matrix to improve the strength and stiffness of the composite is called reinforcements (Blessley, 2002). Reinforcements are always stronger, harder, stiffer than the matrix. Reinforcements can be of different species, ranging from long fibres, particles, flakes, whiskers, sheets, continuous and discontinuous fibres (Garmestani, 1997). Reinforcements are different from fillers, because, while fillers do not increase the strength and stiffness of a composite, a reinforcement does (Blessley, 2002).

Some major materials which can be used as reinforcements are; carbon, metal, glass, ceramics, graphite, boron, synthetic fibres, etc (Blessley, 2002). A strong adhesive bond between the reinforcement and the matrix at the interface helps increase the flexural strength and stiffness (Bunsell, 2001).

Interface

The interface is the common boundary between the fibre and the matrix. The interface is very important in the study of the effective behaviour of composites because it is the surface where there the transfer of load from matrix to fibre takes place.

2.3 CLASSIFICATION OF COMPOSITES

According to Dhakal and Ismail, (Dhakal & Ismail, 2021), composites can be classified into the following components:

- ***Metal-matrix composites;*** contain particulates (fibres) and metal alloys (matrix) as their constituents.
- ***Ceramics-matrix composites;*** contains ceramics(matrix) and Silicon carbide (fibre) their constituents.
- ***Fibre-reinforced polymer composites;*** These composites have their constituents as polymer (thermosets and thermoplastics) as matrix and mostly glass fibres as fibre.

Composites are normally classified based on the constituents that make the composite. As a result of this, classification can be done in two different ways (Blessley, 2002);

- Classification based on matrix constituents.
- Classification based on reinforcement constituents.

Classification Based on Matrix Constituent

Based on matrix constituents, composites can be classified into three:

a) Polymer Matrix Composites (PMC)

b) Metal Matrix Composites (MMC)

c) Ceramics Matrix Composites (CMC)

Polymer Matrix Composites (PMC*):*

Polymers are materials whose large molecules have repeating subunits. Their weight is light, they are very easy to process and they have good mechanical properties. Low strength and stiffness are properties of polymer matrix composites (Campbell, 2010). The types of PMC are:

a) ***Thermoplastics:*** They are those types of polymer matrix composites whose macromolecules are held together by weak forces of attraction. As a result of these weak forces, they melt when heat is applied to them. Despite melting when heated, they tend to return to their original properties when cooled (Warnet & Akkerman, 2009).
b) ***Thermosets:*** These are three-dimensional polymer matrix composites formed by the linking valence bonds between the molecules. When heated thermosets tend to decompose instead of melting (Warnet & Akkerman, 2009).
c) ***Elastomers:*** These polymer matrix composites behave like rubber as a result of weak valence bonds between their molecules. They exhibit more elastic properties than simple plastics (Warnet & Akkerman, 2009).

Metal Matrix Composites (MMC): A metal is characterized by hardness, shiny luster, ductility with good electrical and thermal conductivity. Metal matrix composites are characterized by intermediate strength and stiffness but high ductility. Even though PMC is mostly used more than MMC, they can equally offer better fracture toughness and better protection against corrosion and high temperature than that offered by PMC. Titanium, Aluminium, and magnesium are mostly used as MMC because it is light and has low density, making them a good matrix material (Blessley, 2002).

Ceramics Matrix Composites: Ceramics matrix composites exhibit high electrovalent bonding. They are brittle and can offer good heat and corrosion resistance, are very stable at high temperatures, and possess very good compressive strength but cannot withstand high tensile stress (Blessley, 2002). To increase the load-bearing capacity of CMC, it should be reinforced with high-strength material.

Classification Based on Reinforcement Constituents.

Based on reinforcement, composites can be classified into:

a) Fibre-reinforced composites
b) Laminar Composites
c) Particulates Reinforced Composites

Fibre Reinforced Composites:

Reinforcing fibres has their length far larger or bigger than their diameter. This phenomenon reduces to the minimum the presence of surface defects and accounts for high strength in fibres (Campbell, 2010). The length-diameter ratio (l/d) called *aspect ratio* for any fibre is usually very large and that’s why they can also be called *wires*. Fibres can be divided into two based on their aspect ratio (Campbell, 2010):

- ***Continuous fibres:*** These fibres have a longer aspect ratio and have a particular direction. Examples of continuous fibres are; unidirectional fibres, woven fibres, helical fibres, etc. They have higher strength but are very expensive (Campbell, 2010).

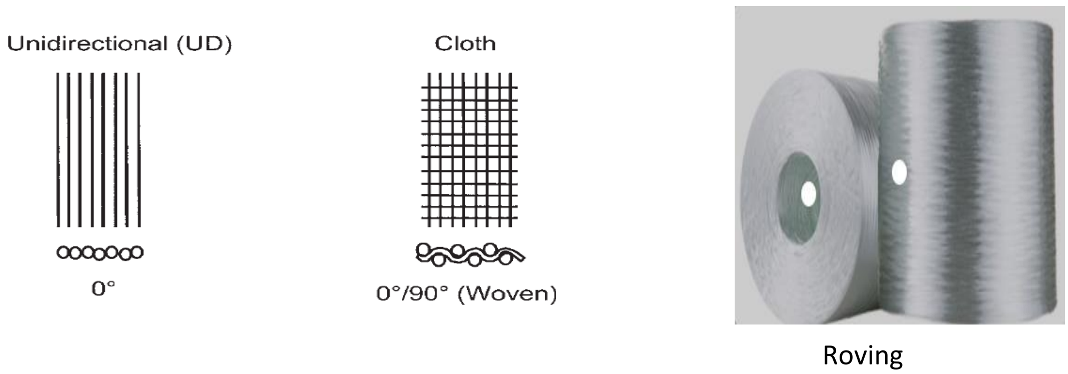

Figure 2.2: Types of Continuous Fibres: *Source:* (Campbell, 2010)

- ***Discontinuous fibres:*** these fibres have a shorter aspect ratio and do not have a particular direction. Examples of discontinuous fibres are; random mat fibre, chopped fibre, etc. They possess lower strength but are less expensive (Campbell, 2010).

Figure 2.3: Types of Discontinuous Fibres: *Source:* (Campbell, 2010)

A good fibre should possess the following properties (Datoo, 1991);

a) A good fibre must have a high Young's modulus in both longitudinal and transverse directions.

b) It must possess high tenacity.

c) It should be uniform in strength, length and thickness in all directions.

d) It should be stable during fabrication.

The efficiency of reinforcing fibre is rated by a couple of factors, namely;

a) Dimension of the fibre.

b) Arrangement and direction of the fibre.

c) Mechanical properties of the matrix.

d) Composition of the fibre.

The strength of a composite material depends greatly on the arrangement and direction of the fibres in the matrix of the material. The arrangement of fibre can be done in both longitudinal and transverse directions, but the strength of a composite is more when the fibre is arranged in the longitudinal direction. To increase the strength of the composite material, fibre reinforcement should be in both directions.

The major composites formed when fibres are used for reinforcements are:

- Glass Fibre Reinforced Composites.
- Carbon Fibre Reinforced Composites.
- Kevlar (Aramid) Fibre Reinforced Composites.
- Boron Fibre Reinforced Composites.

Glass Fibre Reinforced Composites: Glass is an amorphous solid made from silicon oxide used mostly for practical and decorative purposes. Glass fibre composite is a material made with very thin fibres of glass. Glass fibre composites are produced by integrating glass fibres into the polymer matrix (ANITS, 2020). Glass fibres can exist in different forms. They are;

a) (E-glass) fibre: This is the most common type of glass fibre. It is mostly used because it provides good strength and high electrical resistance (Herakovich, Mechanics of Fibrous Composites, 1998).

b) Silica glass (S-glass) fibre: This type of glass fibre is characterized by the high strength it provides. It also provides high modulus and stability under harsh temperatures and corrosive environments (Herakovich, Mechanics of Fibrous Composites, 1998). The only limitation of this S-glass fibre is that the cost of production is high when compared to other forms of glass fibres.

c) C-glass and D-glass fibres: C-glass is characterized by its resistivity to chemical attack and D-glass fibre can be applied in radars (Warnet & Akkerman, 2009).

The merits of glass fibre composite are;

- Resistance to impact, corrosion, and other chemicals
- It is not expensive compared to the strength which it produces.
- Silicon oxide is abundance, glass fibre composites are not scarce
- Production is easy.

- It neither burns nor supports combustion. It retains almost 25% of its initial strength at a temperature of 1000°F (540°C).

Glass fibre reinforced composites does not withstand very high temperature as it tends to fuse. It has a wide range of applications ranging from automobile parts, storage tanks, floorings, plastic pipes (Herakovich, Mechanics of Fibrous Composites, 1998).

Carbon Fibre Reinforced Composites: The pyrolysis of polyacrylonitrile (PAN), rayon, or pitch at a very high temperature gives rise to carbon fibre. The surface structure of carbon fibre depends heavily on fabrication temperature and the processes involved in its production (Herakovich, Mechanics of Fibrous Composites, 1998).

According to (Warnet & Akkerman, 2009), carbon fibres are produced when PAN, rayon, or pitch is oxidized at 400^{o}C and carbonized at 1000 ^{o}C in the presence of nitrogen, carbon fibres are formed. The carbon content of carbon fibre produced is 95%. But when treated at around 1500 ^{o}C, graphite fibre is formed. Graphite have a carbon content of at least 99%.

Carbon fibre reinforced composites are gotten when carbon fibres like graphite, graphene is embedded in a polymer matrix. They have the following properties (Warnet & Akkerman, 2009):

- Carbon fibre-reinforced composites have high corrosion resistance.
- At an elevated temperature, it can retain its behaviour and properties.
- They do not have high densities.
- They possess high Young’s modulus.
- The negative coefficient of thermal expansion
- They are good conductors of electricity.

It finds its application in so many fields like:

- In sports equipment
- Wings and bodies of aircraft

- Fishing rods, etc

Kevlar (Aramid) Fibre Reinforced Composites: Aramid is a plastic organic fibre obtained from the molecules of carbon, hydrogen, oxygen, nitrogen, etc with good resistance to impact (Datoo, 1991). It can also be referred to as an organic fibre from a liquid solution of polymer that exhibits high tensile strength, low compression resistance, and intermediate modulus. (Herakovich, Mechanics of Fibrous Composites, 1998). Kevlar is trade name for aramid by Du Pont.

Polymer is spun into thin threads, during the production of Aramide and then the thin threads are stretched to increase their stiffness. Even though they are difficult to process, they possess good qualities like thermal stability and are very good in energy absorption as they are very ductile (Warnet & Akkerman, 2009).

Boron Fibre Reinforced Composites: Boron fibre is a ceramic fibre obtained by chemically depositing boron vapor on tungsten core or carbon. The fibre produced has a large diameter of approximately $140\mu m$, making it brittle. During fabrication, at room temperature, the composite fibre builds up stress as a result of the difference in the thermal expansion of boron and tungsten (Herakovich, Mechanics of Fibrous Composites, 1998).

They are characterized by lightweight, high strength, and high elastic modulus, and their composites can be found in aircraft components, golf clubs, fishing rods, etc. They are also tough and so can be used in structures like cable and other impact-resisting structures (Bunsell, 2001).

2.4 MECHANICAL PROPERTIES OF FIBRE-REINFORCED COMPOSITES

Consider the elasticity of a continuous and oriented fibrous composite that is loaded in the fibre orientation direction. First, it is assumed that the fibre-matrix interfacial bond is very strong and that both the matrix and the fibres deform in the same way (an iso-strain situation).

The mechanical properties of fibres used to reinforce composites in comparison to the mechanical properties of steel are given in **Table 2.1**. The table showed that despite the small density of these fibres, they possess better strength than steel.

Fibre	Diameter (μm)	Density (Kgm^{-3})	Young's Modulus (GPa)	Tensile Strength (MPa)	Poisson Ratio
E-Glass	16	2600	74	2500	0.25
S-Glass	10	2500	86	3200	0.20
Carbon	7	1750	230	3530	0.20
Kevlar	12	1450	130	2900	0.40
Boron	100	2600	400	3400	0.20
Steel		7800	205	400 - 1600	0.40

Table 2.1: Mechanical Properties of Fibre-Reinforced Composites: *Source:* (Marti'nez, 2008)

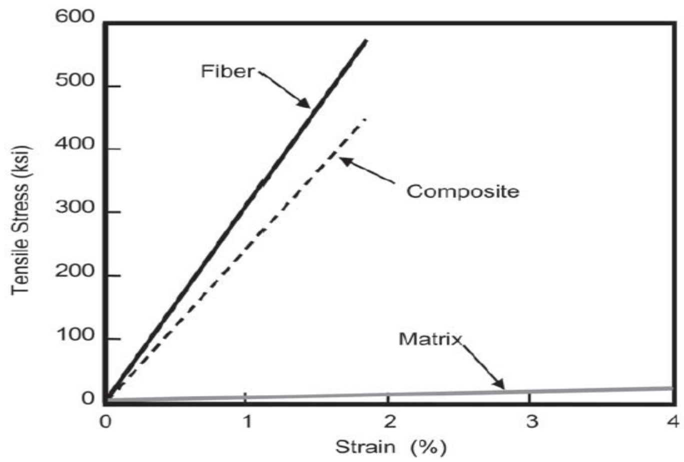

Figure2.4: Stress-Strain Relationship of Fibre, Matrix and Composite. Source: (Campbell, 2010)

Laminar Composites

These are composites formed by the combination of two-dimensional sheets or panels which are arranged in an order of preferred high strength orientation (ANITS, 2020). These composites may be of several layers, in two or more bound together using adhesives and set to occur in a preferred order. The thickness of the individual laminate layer and its arrangement play an important role in determining the effective behaviour and properties of the laminate composite (Herakovich, Mechanics of Fibrous Composites, 1998).

Some sheets, like plastics or metals, may also serve and function as adhesives at room temperature, so may be used to glue two constituents together. A typical example of a laminate composite is plywood.

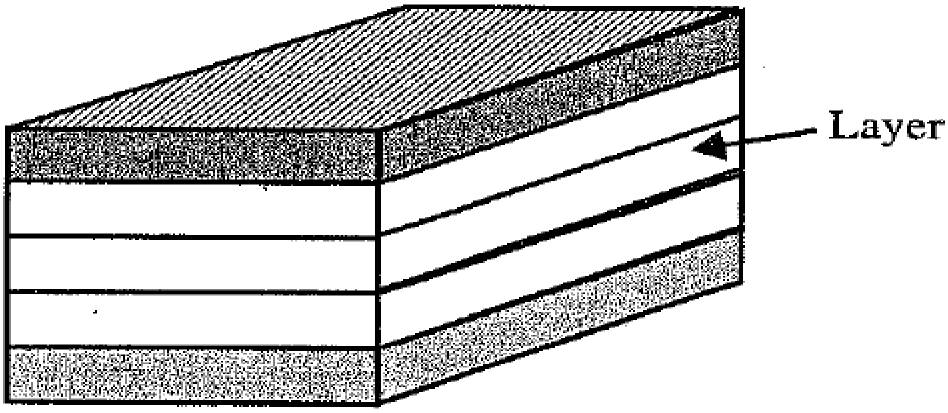

Figure 2.5: Laminate: *Source* (Herakovich, Mechanics of Fibrous Composites, 1998)

Particulate Reinforced Composites (PRC)

Particulate reinforced composites are composites that show the immersion of particles (reinforcements) of different sizes into the matrix of metal alloy, ceramics, polymer, etc (ANITS, 2020). It considers the shapes of the reinforcing particles but assumes that the dimensions are more or less equal. In particulate composites, the reinforcement of the matrix by the particles is through hydrostatic coercion and hardness relative to the matrix.

Particulate composite can be grouped into two;

a) ***Large Particulate Composites;*** This composite, works with all types of material, be it metal, ceramics, or plastics. For example; cement (matrix) is strengthened by aggregates (particles) to form concrete (composite). Also, Tungsten-carbide (particulate) immersed in Cobalt (matrix) forms a composite that requires surface hardness.

b) ***Dispersion Strengthened Composites;*** This composite works with very small particles as reinforcements. The size of the particles ranges from 10mm to 100mm. This method uses a high percentage of a very hard and inert metal as reinforcing particles. The gain in strength is through the interaction between particles and voids within the matrix in the presence of appropriate heat.

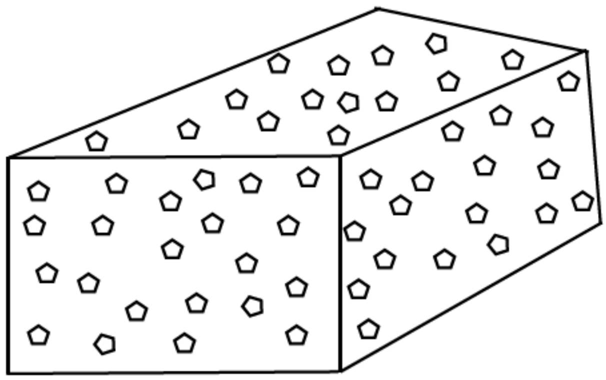

Figure 2.6: Particulate Reinforced Composites (PRC): *source: (Herakovich, Mechanics of Fibrous Composites, 1998)*

As a result of improved strength in fibre-reinforced composites, it is preferred because it reduces the number of irregularities present in the material when it is in bulk form (Barberto, 2011). Shashi Bahl, (Bahl, 2021), said that the properties of the fibre-reinforced composite are a function of its matrix material, nature of the fibre, the direction of the fibre, and the length of the fibre. Fibre-reinforced composites find their application in space shuttles, automobiles, golf bats, bicycles, electronic substrates, etc

To design a composite structure, one can use the analytical or numerical method. The analytical method involves solving a problem by the idealization of the given structure. This method can only solve simple structures. So, to design a complex composite structure, the best method is the numerical approach. This approach is always referred to as Finite Element Analysis (FEA) or Finite Element Method (FEM).

Finite Element Analysis (FEA) is a numerical method for solving problems in engineering and mathematical physics that involve complicated geometries, loadings, and material properties and for which analytical solutions are difficult to find (Lectures). Because of the complexity of FEA design, it necessitates a thorough understanding of how the complex structure functions, its flaws, and its ideal design confidence (Lectures). For complicated stresses, complex geometries and numerical solutions, the best method of analysis is the FEA. (Jagota, Sethi, & Kumar, 2013)

To analyze and obtain the effective behaviour and characteristics of a composite is the aim of this chapter. This can be done in two scales;

- ***Micro-Mechanical Scale:*** The heterogeneous scale of analysis is a common name for this scale. This is because structures on this scale often change predictably from one point to another and entail investigating the structural features of constituents independently (Datoo, 1991).
- ***Macro-Mechanical Scale:*** The homogeneous scale of analysis is a common name for this scale. This scale analyses a composite's entire body and its properties as a whole (Datoo, 1991). Macroscale modelling represents an effective strategy to describe the response of composite material under different loading conditions.

Even though the thermo-mechanical behaviour of a structure can be determined by asymptotic homogenization, recent developments in the field of engineering such as mathematical modelling which analyzes the framework of the Representative Volume Element (RVE) gives approximate solutions to the geometry of the microstructure (Terada, Hori, Takashi, & Kikuchi, 2000).

2.5 THE REPRESENTATIVE VOLUME ELEMENT (RVE)

RVE is a micromechanics concept that aids in determining the functional behaviour of composites by utilizing the qualities of the microstructure's micro components. The idea of RVE is employed in most methodologies for analyzing or obtaining the functional behaviour of a composite structure. The RVE model is used to depict the composite's microstructural scale, which is believed to be heterogeneous. The length scale is supposed to be large enough to represent the heterogeneity of the composite at the microscale and small enough to represent the homogeneity of the composite at the macroscopic scale, based on the separation of scales.

According to (Drugan & Willis, 1996), the definition of RVE is categorized into two;

- Firstly, the RVE is defined as a model representing all possible configurations of the inhomogeneities in the microstructure of the composite.
- Secondly, the RVE is defined as the smallest volume of the macroscopic model which represents all functional behaviour of the composite.

From the definitions above, it is clear that the first definition will make the RVE have a large size since it will have the inhomogeneities of the microstructure, while the second one will lead to a smaller RVE size. As a result of the above definitions, it can be said that the minimum size of the RVE is a function of the properties of the constituents of the composite and the loading on the macroscopic scale (Kouznetsova V. G., 2002). Thus, to get a good functional behaviour of a composite structure, with different boundary conditions, then there should be an increment in the size of the microstructural cell.

The result gotten from analyzing the RVE is always incorporated in the macroscopic scale to obtain the homogenized functional behaviour of the composite. Therefore, to get accurate modelling of a composite structure, the proper RVE is to be chosen.

In this method, the separation of scales condition is usually applied. Separation of scales condition talks about the size of the RVE which should be larger than the size microscopic scale and smaller than the macroscopic scale size (Beluch & Hatlas, 2018). This relation is shown thus:

$$\boldsymbol{l_m} \ll \boldsymbol{l_R} \ll \boldsymbol{l_M}$$

To analyze these composite structures is not always easy as most times they exhibit nonlinear behaviour. The methods that can be used to analyze and solve for the effective and functional behaviour of composite structure are;

1. Micromodel methods
2. Mixing theorem
3. Homogenization method

2.6 MICROMODEL METHOD

The micromodel method can also be called micromechanics because it analyzes a composite structure at its constituent level. Showing the functional behaviour of the constituents of the composite structure in an organized and contentious way is the major aim of the micromodel method. It analyzes a composite structure by modelling its microstructure.

It can prognosticate the functional behaviour of a composite as a result of the properties, arrangement, and volume fraction of the constituents of the composite structure (Herakovich, Mechanics of Fibrous Composites, 1998). Micromodels study the interatomic bounding of the constituents in the microlevel of the composite (Car, Zalamea, Oller, Miquel, & Onate, 2002; Oller, Oñate, Miquel, & Botello, 1996). It can get the solution to some effects like contact, stress, and strain, detect debonding between fibre and matrix, detect cracking (Otero, Oller, Martinez, & Salomón, 2015). Micro modelling answers are closer to real conditions than macro models, thereby making them more suitable for detecting failure mechanisms (Goda, Váradi, & Friedrich, 2001).

Violeau, et al., (Violeau, Ladevèze, & Lubineau, 2009) developed a microscopic model which is used in the simulation that estimated for damage in laminated composites. In the microscopic analysis of composite structure, the microstructure is assumed to be heterogeneous, i.e. to say that within the infinitesimal locality, the composite has a complex structure, which leads to the introduction of RVE (Nemat-Nasser & Hori, 1993). Also, (Drugan & Willis, 1996) formulated equations to derive the micromechanics-based equations for linear elastic composite structure.

RVE is a concept of micromechanics that helps in determining the functional behaviour of the composites using properties of the micro constituents of the microstructure.

One of the limitations of this model is its computation time. The computation time is very expensive. Another limitation is that the use of micro models is not practical.

2.7 MIXING THEOREM

The mixing theory or classical rule of the mixture is one of the several theories used for solving or simulating both the functional linear and nonlinear behaviour, properties, or performance of a composite structure. It is a method that gives the solution to a composite structure as a result of the relationship between the constituents that makes up the composites. A mixing theorem is an approach to composite material simulation because it does not consider the micromechanical constituent of the composite structure during simulation. Even without the consideration of the microstructure of the composite material, it prognosticates the functional behaviour of the composite materials with its nonlinearity efficiently at a low computational cost. In this theory, the composite's topological distribution is used to determine its mechanical characteristics.

The classical mixing theorem was first formulated by (Trusdell & Toupin, 1960). Their formulations lead to further discoveries. Ortiz & Popov, (Ortiz & PoPov, 1982; Ortiz & Popov, 1982) applied the formulations of Trusdell & Toupin to demonstrate that when a load is imposed on concrete as a composite structure, tensile tension exists in the mortar. Green & Naghdi (Green & Naghdi, 1965) made use of Trusdell & Toupin formulations to discuss the thermodynamics of each constituent in terms of mass, momentum, energy balance, and so on. Also, an effective mixing theorem, provides the nonlinear mechanical behaviour of composite material and extends it to multiphase materials. Sergio Oller, (Oller S. , Numerical Simulation of Mechanical Behavior of Composite Materials, 2014) modified the classical mixing theory formulated by Trusdell & Toupin, by generalizing the mixing theory. This generalization states that the strain on a composite is a result of the sum of the individual strains from all constituents of the composite in parallel and series directions. Martinez, et al (Martinez, Oller, Rastellini, & Barbat, 2008), used the serial/parallel rule of the mixing theory in the simulation of a composite structure. This method applied iso-strain strain conditions when the fibre direction is in the series direction with the matrix but uses iso-stress when the fibre direction is in parallel with the matrix. This iso-stress condition is also called the *Inverse Mixing Theory.*

The classical mixing theorem was achieved using the following hypothesis;

1. All of the composite structure's constituents are present in a microscopic volume of the composite.
2. The contribution of each constituent to the actual behaviour of the composite structure is proportional to its volume.
3. There is a particular strain on all of the constituents of the composite.
4. When compared to the volume of the composite, each constituent occupies a smaller volume.

The first two hypotheses are concerned with the uniform or even distribution of all composite constituents at any position on the composite material (Linero, Oliver, & Huespe, 2007). The third hypothesis shows that there is the same strain amongst the constituents that made up the composite structure (Car, Zalamea, Oller, Miquel, & Onate, 2002) whereas the last hypothesis gives the compatibility equation of the constituents of the composite (Linero, Oliver, & Huespe, 2007).

The composite's material free energy is the sum of each free energy of the constituents which is based on the volume of each constituent participating (Trusdell & Toupin, 1960).

One limitation of the mixing theorem is that its validity holds only when all the constituents of the composite structure are either compressible or incompressible. This is because the compatibility condition in the hypothesis will not hold if any of the constituents are either compressible or incompressible (Car, Oller, & Oñate, An anisotropic elastoplastic constitutive model for large strain analysis of ®ber reinforced composite materials, 2000).

2.8 HOMOGENIZATION THEORY

The relationship between mechanics and material science has been strengthened through multi-scale approaches (Geers, Kouznetsova, & Brekelmans, 2010; Geers, Coenen, & Kouznetsova, 2007). Multiscale as the name implies shows that this method will involve different dimension scales when analyzing a composite structure. The analysis will be in such a way that the result from one of the scales will be shared amongst the scales involved, which will help in analyzing the other scales. In other to predict how these composites respond, the use of a multi-scale modelling approach is also used (Tikarrouchine, Benaarbia, Chatzigeorgiou, & Meraghni, 2021). Contrary to analytical approaches, multiscale techniques are favoured for simulations with significant discrepancies in material science and engineering, such as composite materials, porous media, turbulent flow, and so on (Efendiev & Hou, 2009).

Homogenization theory is one of the formulations that is used to estimate the behaviour and properties of a composite structure. It works by dividing the structure into two scales. These scales are the macroscopic scale and the microscopic scale. In the macroscopic scale, the composite is assumed to be homogeneous, while the microscopic scale is assumed to be heterogeneous. At the microscopic level, a unit heterogeneous volume represents the composite. The homogenization process allows the substitution of a heterogeneous structure with a homogeneous model while solving for the properties and behaviour of the composite structure (Nguyen, Stroeven, & Sluys, 2011).

Classification of Homogenization Process

According to Nguyen (Nguyen, Stroeven, & Sluys, 2011), there are three categories of homogenization, namely;

1. Analytical Homogenization
2. Numerical homogenization
3. Computational homogenization

Analytical Homogenization

Analytical homogenization prognosticates the behaviour of a periodic microscopic structure and can also be used to deduce the behaviour of a large or sizable non-periodic composite structure. (Chen & Schuh, 2009). A periodic composite has its phase arranged rhythmically within its unit cell.

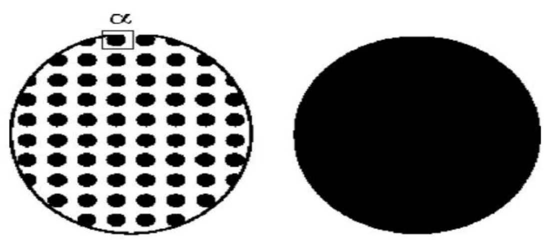

Fig2.7: (a) Periodic composite material (b) Same material when the periodicity α.
Source: (Ouchetto, Qiu, Zouhdi,, Li, & Razek, 2006)

In the previous years, the complexity and heterogeneity of composite structures have been studied by Sanchez-Palencia (Sanchez-Palencia, 1980) and Bensoussan (Bensoussan, Lions, & Papanicolaou, 1978), as they developed an analytical method called asymptotic homogenization. The asymptotic homogenization precisely analyses the behaviour of a composite structure by solving for the behaviour of an equivalent homogeneous model instead of the original heterogeneous structure. It solves for effective behaviour, local stress, and strains in the microscopic structure of a composite with great precision. (Kalamkarov, Andrianov, & Danishevs'kyy, 2009). An analytical method of homogenization was used by (Shu & Stanciulescu, 2020) to solve precisely the behaviour of fibre-reinforced composites whose interface is imperfect.

The analytical method for getting the functional behaviour of a periodic composite material can be done with the use of Fourier space (Kalamkarov, Andrianov, & Danishevs'kyy, 2009).

As an example of analytical or mathematical homogenization, asymptotic homogenization has its limitations, which is its ability to model only the effect of small strains on simple microscopic geometries.

Numerical Homogenization

Numerical homogenization models a macroscopic sample using data gotten from finite element fitting of an explicitly modeled microstructure of a microscopic sample (Nguyen, Stroeven, & Sluys, 2011). Numerical homogenization aims at getting the effective properties of an RVE without solving the fine-scale problems (Efendiev & Pankov, 2004; Antoine, 2012). It computes not only the main or the functional macroscopic behaviour such as the elasticity tensor (Andreassen & Andreasen, 2014) but also some alteration or nonlinear effects in the microscopic scale, like contact, debonding damage plasticity, etc (Drosopoulos, Wriggers, & Stavroulakis, A multi-scale computational method including contact for the analysis of damage in composite materials, 2014), which may be important in many applications. It can also solve partial differential equations from the inhomogeneity of a structure (Antoine, 2012). According to Beluch & Hatlas, (Beluch & Hatlas, 2018), numerical homogenization solves the functional differential equations applied to a higher scale and the relationship between field variables, like stress and strain.

Dascalu, et al., (Dascalu, Bilbie, & Agiasofitou, 2008) used microstructural analysis to solve for the micro-mechanical damage for solid models. Michel, et al., (Michel, Moulinee, & Suquet, 1999) also compared the use of Fast Fourier Transform (FFT) and Finite Element Method (FEM) as a means of numerical homogenization used to analyze composites with periodic microstructure. Two methods involved in numerical homogenization are RVE/unit cell method and Wave propagation method.

RVE Method: This RVE or unit cell is assumed to have a very small dimension microstructure when compared to the macroscopic dimensions of the structure.

The procedures for the numerical homogenization works by (Li, Zhang, Chang, Liu, & Li, 2015) can be summarized as:

- Choice of suitable RVE or unit cell method;
- The division into elements and obtaining the nodal coordinates and elemental connectivity;
- Creation of shape functions;
- Establishing the boundary conditions at the edges and nodes of the RVE;
- Application of boundary conditions on the nodes of the RVE
- Solving for the properties of the microstructure the same way as in the standard FEM;
- If a triangular or tetrahedral element is used, it can be modified to suit the shape.

Wave Propagation Method: This method makes use of a wave vector to find the connection between the nodes of the adjacent cells which are separated by one period to find the boundary conditions between them (Lenglet, Hladky-Hennion, & Debus, 2003). Also changing the direction and magnitude of the wave vector provides details of the dispersion curve, mode of propagation pass, and stop bands (Lenglet, Hladky-Hennion, & Debus, 2003).

Numerical homogenization has some limitations. One of the limitations of this method is that it is not suitable for nonlinear problems with evolving microstructures because the constitutive material law of the macroscopic structure is always assumed (Nguyen, Stroeven, & Sluys, 2011). Another limitation is its inefficiency in handling incompressible materials (Li, Zhang, Chang, Liu, & Li, 2015).

2.9 COMPUTATIONAL HOMOGENIZATION

The best technique which gives an accurate solution in upscaling the nonlinear behaviour of a well-characterized microstructure among various homogenization techniques is computational homogenization. (Geers, Kouznetsova, & Brekelmans, 2010). To get the approximate solution to some partial equations, which shows the behaviour of a complex structure derived by discretization at the nodes, using FEA, is the major aim of computational mechanics. (Atsuya Oishia & Genki Yagawa, 2017). Computational homogenization aims at providing a model of a composite material whose effective behaviour can be solved using a Finite Element program in software like MATLAB (Yvonnet, 2019).

The theory of computational homogenization can be summarized in the following steps as presented by (Suquet, 1985);

a. Definition of RVE which should contain all constituents at the microscopic level and still represent the effective properties at the macroscopic level of the composite structure.
b. Formulation of macro-to-micro transition using the averaging theorem.
c. Using the result from the deformed RVE at the microscopic level to solve for the unknowns at the macroscopic level.
d. Relating the results from the microstructure to the results in the microstructure.

A lot of authors have discussed computational homogenization in the past. Authors like (Suquet, 1985), summarized the steps involved in computational homogenization. Considering the microstructure of a composite structure, (Guede & Kikuchi, 1990) used computational homogenization to solve for the elastic constants of the composites. Later, (Terada & Kikuchi, 2001) proposed a unified way of solving for the behaviour of a heterogeneous media whose microstructure is fine and periodic using computational homogenization. Miehe & Koch, (Miehe & Koch, 2002) investigated how microstructures behave when small strains act on them by calculating for the homogenized stresses and tangent moduli.

Some authors have applied the use of computational homogenization in various fields of study. For example, Patel & Zohdi, (Patel & Zohdi, 2016) applied the use of computational homogenization in the design of effective electromagnetic properties for linear isotropic composites made with ellipsoidal particles. Another application was by (Schröder, Labusch, & Keip, 2016), who used computational homogenization in modelling the interactions between the magnetic, electrical and mechanical quantities in a magneto-electric-mechanically coupled composite structure. It was used by (Escoda, Willot, Jeulin, Sanahuja, & Toulemonde, 2011) to predict the behaviour of Three-Dimensional (3-D) mortar images. In dynamics, computational homogenization was used by (Krushynska, Kouznetsova, & Geers, 2014) to analyze the behaviour of acoustic metamaterials with locally resonant behaviour which was coated with rubber.

There are two kinds of computational homogenization, namely;

- First-Order computational Homogenization
- Second-order Computational Homogenization.

First-Order computational Homogenization

The advantage of this type of computational homogenization is that, during simulation, computational homogenization builds the macroscopic material laws numerically, thereby solving the microscopic problems, and the results transferred to the macro-scale (Drosopoulos, Giannis, Stavroulaki, & Stavroulakis, 2018), i.e to say that there is no assumption of the material properties of the composite before simulation. Other advantages of computational homogenization can be summarized thus:

a) Computational homogenization can be used to study non-linear effects like contact, debonding, damage, and plasticity (Drosopoulos, Wriggers, & Stavroulakis, A multi-scale computational method including contact for the analysis of damage in composite materials, 2014). So, whenever the geometry, mechanics, or physics of a microstructure is complex, computational homogenization is the right tool for the analysis of such structure (Geers, Coenen, & Kouznetsova, 2007).

b) It does not describe the inhomogeneities of the composite structure at the macroscopic level (Yvonnet, 2019).

c) Large stresses and rotations can be handled by computational homogenization, which is a limitation of analytical homogenization.

d) It maintains consistency and stability in its results by switching between the two scales involved at all times.

e) Using either actual data or specifics about the qualities of the idealized constituents of the composite structure's microstructure, computational homogenization can improve, optimize, and evaluate the main behaviour of a composite material (Yvonnet, 2019)

Basic Assumptions of First Order Computational Homogenization

Firstly, the composite material to be analyzed is assumed to be homogeneous at the macroscopic level and assumed to be heterogeneous at the microscopic scale. Considering the length scale, and continuum approach, the length scale at the microscopic level is bigger than the length scale of the molecules of the constituents.

In computational homogenization, it is assumed that at every gauss point in the macroscale, the microstructure has a different pattern that repeats within the small domain of the individual points on the macroscale.

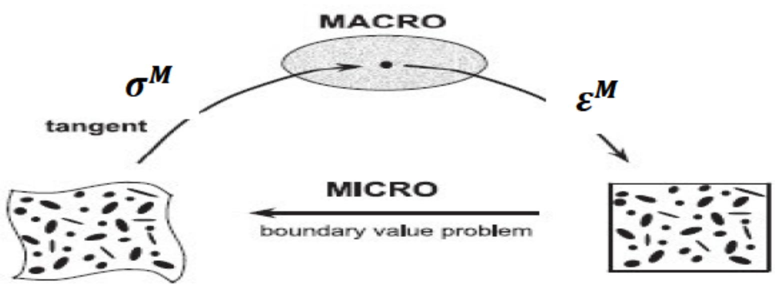

Figure2.8: First-Order Computational Homogenization Scheme. *Source:* (Kouznetsova V. G., 2002)

The procedure for computational homogenization shown in this work is deformation driven (Kouznetsova V. G., 2002). The procedure is summarized as follows:

In the first-order computational homogenization, the RVE is loaded with a loading strain, (macroscopic strain), $\boldsymbol{\varepsilon^M}$**.** This loading which is done at every gauss point on the macroscopic scale is used to generate the boundary condition conditions which are to be imposed on the boundaries of the RVE.

The microscopic stress, $\boldsymbol{\sigma^m}$of the RVE is utilized to determine the macroscopic stress, $\boldsymbol{\sigma^M}$, when simulations and solutions to the RVE's boundary value issues are received, using the Hill-Mandel volume averaging theorem (Hill, 1963).

The macroscopic strain, $\boldsymbol{\varepsilon^M}$ and the macroscopic stress, $\boldsymbol{\sigma^M}$ are now used to calculate the consistent tangent stiffness, $\boldsymbol{C^M}$ depending on the response of the microstructure.

The limitations of this method as given by (Geers, Kouznetsova, & Brekelmans, 2010) are summarized as;

a) It is unable to work on a macroscale with huge spatial gradients due to the principle of scale separation, which imposes size constraints.

b) It does not take physical size into account; hence it cannot accurately simulate a composite whose macro-behaviour is influenced by size.

c) At the macroscale, it is solely applicable to normal continuum mechanics theory.

But despite the above limitations, it has been proven to be a reliable and flexible method of solving for the effective mechanical behaviour of nonlinear heterogeneous composites which have been used by so many authors even beyond its limits of application. In chapter 3, which is the methodology, this method will be discussed in detail as it was the method used in this research.

Second-Order Computational Homogenization

The second-order computational homogenization is an improved version of the first-order computational homogenization. This improvement is mainly to salvage the major limitation of the first order homogenization by integrating the length scale which is determined by the RVE size. As an improved method, it can solve most things that the first-order computational homogenization cannot do, ranging from problems with size effects and that of high localized deformation.

In (Bacigalupo & Gambarotta, 2010), a second-order computational homogenization procedure with superposition is used to express a polynomial which relates micro-displacement, macro-displacement fields, and micro fluctuations serving unknowns for the inhomogeneity effects. A gradient enhanced computational homogenization procedure was proposed by (Kouznetsova, Geers, & Brekelmans, 2002) to model RVE microstructural size effects. Furthermore, (Kaczmarczyk, Pearce, & Bic´anic´, 2010) used second-order computational homogenization with examples to show the effect of microstructural size effect and higher-order deformation.

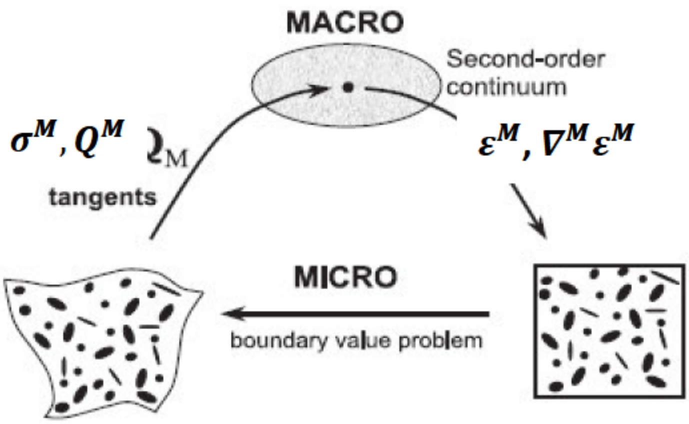

Figure2.9: Second-Order Computational Homogenization Scheme. *Source:* (Kouznetsova V. G., 2002)

Two bounds strictly control the choice of the RVE size in second-order computational homogenization (Geers, Kouznetsova, & Brekelmans, 2010), namely;

a) ***Upper bound***: This bound considers linear variation in macroscopic strain fields and quadratic variations in the macroscopic displacement fields over the size of the RVE.

b) ***Lower bound*****:** This bound is governed by the boundary conditions and the statistical analysis of the RVE, just like the first-order computational homogenization.

In this type of computational homogenization, the periodic boundary condition which is applied on the RVE is imposed by macroscopic loading strain (macroscopic deformation tensor), $\boldsymbol{\varepsilon}^{\boldsymbol{M}}$ and the macroscopic gradient tensor, $\boldsymbol{\nabla}^{\boldsymbol{M}}\boldsymbol{\varepsilon}^{\boldsymbol{M}}$. After the simulation has been completed and the boundary value problem of the RVE has been solved, the macroscopic stress tensor, $\boldsymbol{\sigma}^{\boldsymbol{M}}$ as well as the higher-order stress tensor,$\boldsymbol{Q}^{\boldsymbol{M}}$ can be calculated using a modified Hill-Mandel averaging relation. This shows that without much assumptions on the macroscopic scale, the higher-order stress tensor is extracted from the microstructure using the second-order computational homogenization (Kouznetsova, Geers, & Brekelmans, 2004).

The advantages of second-order computational homogenization as given by (Geers, Kouznetsova, & Brekelmans, 2010) can be summarized thus:

a) It considers the length scale at the microscale RVE.
b) In the case of localization in the macroscale, second-order computational homogenization can solve the ill-posed problems.
c) This method can be employed to solve gradient-sensitive material at the microscale.
d) This method solves second-order equations from a lower scale.

Despite the above advantages of this method, its inability to be used for complete softening analysis at the macroscale is a limitation to second-order computational homogenization.

2.10 DEBONDING BETWEEN CONSTITUENTS OF A FIBRE-REINFORCED COMPOSITE

The major constituents of fibre-reinforced composite materials are the matrix and the fibre. The boundary surface between the two constituents is called interface and it helps in load transfer from matrix to fibre (Le, Dau, Pham, & Tran, 2021). The knowledge of the performance of the interface of the constituents helps design technical systems with the composites (Wriggers P. , 2006). The mechanical behaviour of composite material is also a function of the interfaces between the constituents of the composite structure (Paggi, Carpinteri, & Zavarise, 1949).

It is always assumed that a perfect bonding between the constituents of a fibre-reinforced composite is the major determinant of its behaviour but the presence of heterogeneities such as voids can heavily influence the behaviour of the composites (Benveniste & Aboudi, 1984; Georgiadis, Stavroulak, Koltsakis, & Panagiotopoulos, 1990).

2.11 DATA-DRIVEN MULTISCALE HOMOGENIZATION

Computational homogenization solves nonlinear problems in composite structures but because of its high cost of computation time, other methods like the data-driven approach of the simulation were initiated. This data-driven approach in many cases solves the microscale problems offline and then the result is used online as data to solve for the effective behaviour at the macro-macroscale (Lu, Yvonnet, Papadopoulos, Kalogeris, & Papadopoulos, 2021; Lu, et al., 2018).

Data-driven computational homogenization is a growing field in science, engineering, and computational mechanics. This is because problems that relate Data Science to material science and engineering have not been investigated and utilized properly (Conti, Müller, & Ortiz, 2018). Unlike in the past where data is scarce, recently, data is abundant as a result of advances in experiments in science and multiscale computing. Data-driven analysis aims to find the closest compactable strain field and balanced stress field from the material dataset.

A data-driven model is a scientific model which redesigns the traditional initial boundary value problems directly from material data (Conti, Müller, & Ortiz, 2018). According to (Kirchdoerfer & Ortiz, 2016), data-driven is a new pattern developed to analyze a composite structure by calculating directly from the experimental material data, conservation laws, and pertinent constraints.

Data-driven makes use of raw data from real observation as an objective step to the learning experience (Montáns, Chinesta, Gómez-Bombarelli, & Kutz, 2019). Compared to a classic finite element analysis (FEA), the data-driven FEM leads to a modified calculation problem. The essential equilibrium laws and equilibrium equations must be solved, and regardless of this, the deformation kinematics must be compatible (Korzeniowski & Weinberg, 2021). Composite structures, geometrical nonlinearity, dynamics, elasticity with noisy material data set, etc, are among the parameters which can be solved with data-driven computation (Xu, et al., 2020).

According (Montáns, Chinesta, Gómez-Bombarelli, & Kutz, 2019), the reasons for adopting data-driven in study of composites can be summarized as:

a) The simulations of complex solids and analysis of non-linear solids have led to large computational power.
b) There is availability of limited data for many materials which are gotten from testing and observations under different conditions
c) There is an availability of models which can store information and use it to build specific solutions at any given time.

So many authors have written a lot on the applications of data-driven computational homogenization. Some authors like (Waseem, Heuzé, Geers, Kouznetsova, & Stainiera, 2021), adopted an enriched continuum that captures diffusional phenomena in heterogeneous materials using a data-driven reduced homogenization method. This method unveils a history-dependent non-Fickian behaviour on the macroscopic scale. Also, (Karapiperis, Stainier, Ortiz,

& Andrade, 2021), presented a data-driven framework for multiscale mechanical analysis of materials that predicts the behaviour of the material when it is loaded along complex nonmonotonic loading paths. Furthermore, (Siddiq, 2020), presented a data-driven finite element method that accounts for more than two material state variables, capturing the strain rate dependency deformation, material anisotropy, degradation, and failure. Even (Zhang & Garikipati, 2020), worked with a multi-component crystalline microstructure using data-driven to predict its mechanical free energy and homogenized stress-strain response generated based on the computational framework.

Many authors have used the data-driven multiscale homogenization approach in combination with Neural Network in the analysis of composite materials. In (Lu, Yvonnet, Papadopoulos, Kalogeris, & Papadopoulos, 2021), a stochastic data-driven finite-element (FE^2) was used for multiscale calculations using a hybrid neural network interpolation (NN-I) in which the results gotten from RVE calculations was used as inputs in other to model the macroscopic constitutive law. Also, (Avery, Huang, He, Ehlers, & Derkevorkian, 2021) researched several regression methods coupled with Artificial Neural Network, ANN which can solve homogenization problems of hyper-elastic woven composites.

Applications of Data-Driven Procedures.

The summary of the applications of data-driven procedures as presented by (Montáns, Chinesta, Gómez-Bombarelli, & Kutz, 2019) are;

- It is used to monitor and predict things in the processing industry.
- It is used by earth scientists and engineering to model.
- To improve the accuracy of turbulence in fluid dynamics when using Reynolds Averaged Navier Stokes (RANS)

- Crowd simulation can also be improved with the use of data-driven procedures
- Data-driven procedures generate a meaningful prediction from a relatively small amount of data present.

2.12 ARTIFICIAL NEURAL NETWORK (ANN)

Artificial Intelligence, Machine learning, and deep learning methods have found their way into engineering and material science (Xiao, Deierling, Attarian, & El Tuhami, 2021). Artificial Intelligence and cognitive science gave birth to Machine learning (Skansi, 2018). Artificial neural network, Gaussian process regression, polynomials. etc., are flexible machine learning tools (Zimmerlinga, Dörr, Henning,, & Kärger, 2019). Image and speech recognition, as well as language processing, have been a success in engineering fields because of machine learning (Liu, Tain, Tao, & Yu, 2021). To reduce the complex nature of the model, data-driven models such as machine learning, deep learning, and artificial neural networks are used (Aldakheel, Satari, & Wriggers, 2021).

There are four terms that best describe a neural network (NN). They are;

- Data set
- Model
- Loss function
- Optimization procedure

DATA SET: This is the total information which the NN uses to train an algorithm, validate an algorithm, and test an algorithm (Aldakheel, Satari, & Wriggers, 2021). These data set can be an experimental set of data or the one gotten from simulations. The data set is divided into three;

- ***Training set:*** The algorithm learns during training using the training data set. Usually, 70% to 80% of the data set is used for the training. The outputs of a NN are approximated by training the data set.
- ***Validation data set:*** This data set is used to estimate what the algorithm has learned after the training. Usually, 10% to 15% percent of the data set is used for validation.
- ***Testing data set:*** This data set checks the efficiency of the training. Usually, 10% to 15% percent of the data set is used for testing.

MODEL: This is the informative representation of the structure which is being described by the trained algorithm.

LOSS FUNCTION: Loss function is the standard function that was minimized during the training algorithms (Aldakheel, Satari, & Wriggers, 2021). Loss function defines a goal against which the model's performance is evaluated, and the parameters learned by the model are determined by minimizing a chosen loss function

OPTIMIZATION PROCEDURE: This is a method used in obtaining the variables of the model which helps in minimizing the loss function (Andreassen & Andreasen, 2014).

An artificial Neural Network is a computing system inspired by the biological neural network of the human brain. According to (Wilson, 2012) "*An artificial neural network is a collection of simple artificial neurons connected by directed weighted connections*". According to (Balokas, Czichon, & Rolfes, 2018), a mathematical model that is based on the biological nervous systems which learn about its environment through training is called Artificial Neural Network (ANN) or simply Neural Network (NN).

ANN is constructed to solve problems through learning and can solve problems like pattern recognition, prediction, optimization, and clustering (Lu, et al., 2018). It has been used by so many authors to solve problems in so many fields. ANN has gained popularity in modelling composite materials because it approximates a complex nonlinear relationship, and advanced open-source libraries (Liu, Tain, Tao, & Yu, 2021). Because ANN has a good performance with growing data and approximates complex nonlinear simulations, it is considered the best technique for the simulation of composite structures (Liu, Tain, Tao, & Yu, 2021). ANN can either be used to simulate a material or identify the variables of a model (Unger & Könke, 2008).

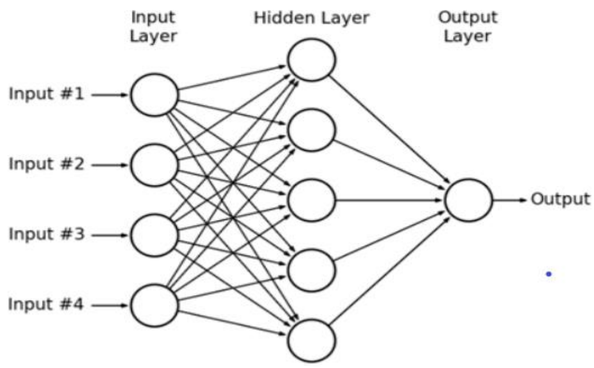

Figure 2.10: The Structure of a Simple Neural Network: *source* (Aldakheel, Satari, & Wriggers, 2021)

From ***Figure 2.10***, a simple ANN structure consists of three layers;

- ***The Input Layer:*** This is where the inputs for the simulation are stored.
- ***The Hidden Layer:*** This is where most calculations are done.
- ***The Output Layer:*** This shows the result of the simulation.

The three layers contain an element that holds information. This element is called a *neuron. Weight* is a parameter that shows the quantity transmitted from one layer to another. The magnitude of the weight does not have a boundary, so it can increase or decrease the value of the next neuron. From ***Figure 2.10,*** it is seen that every neuron of one layer is connected to all neurons of the next layer but neurons in a layer are not interconnected. The neurons from one layer to another get multiplied by weight before transmission. For example, if the input is 15 and the weight to the destination neuron is 0.3, then the destination value will be 3.

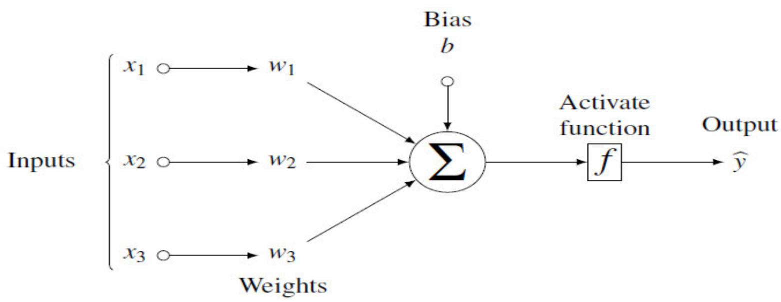

Figure 2.11: Structure of an Artificial Neuron. *source:* (Aldakheel, Satari, & Wriggers, 2021)

From ***Figure 2.11***, it is shown that the neuron labeled $\boldsymbol{\Sigma}$, has a modifiable value called *bias.* The result is always added to the product of the weight and inputs before transmitting to the next layer. This sum is called *logit.*

Information always flows from the input layer through the hidden layer to the output layer. The major and the only function of the first layer (input layer) is the acceptance of inputs. And each neuron in the input layer is assigned to a particular input. Inputs can be represented as a row vector, (1,2,3,4) or as a column vector $(1,2,3,4)^T$. The choice of representation is a function of that representation that will make the algorithm easier and faster to compute. The following need to be present to give full information about a NN. They are;

- The number of layers present in the NN.
- The size of inputs is equivalent to the number of neurons in the input layer.
- The number of hidden layers.
- The number of neurons in the hidden layers.
- Initial values of the weights.
- Initial values of the biases.

From ***Figure 2.11***, the relation for the output is;

$$\hat{\boldsymbol{y}} = \boldsymbol{f}\left(\sum_{\boldsymbol{i}=\mathbf{1}}^{\boldsymbol{N}}(\boldsymbol{x_i w_i} + \boldsymbol{b})\right) \qquad \textbf{(2.9)}$$

The output of the neurons, the efficiency of computation, and the ability of the model train are determined by the activation function, $\boldsymbol{f}$ of the neural network (Aldakheel, Satari, & Wriggers, 2021). The two major types of activation function are:

- **Linear Activation Function:** This function has an infinite number of points in its range and does not have any effect on the complex nature of the data set (Aldakheel, Satari, & Wriggers, 2021). An example is the Purelin activation function. It is represented mathematically by the equation:

$$\boldsymbol{f(x) = x;\ f^{1}(x) = 1} \tag{2.10}$$

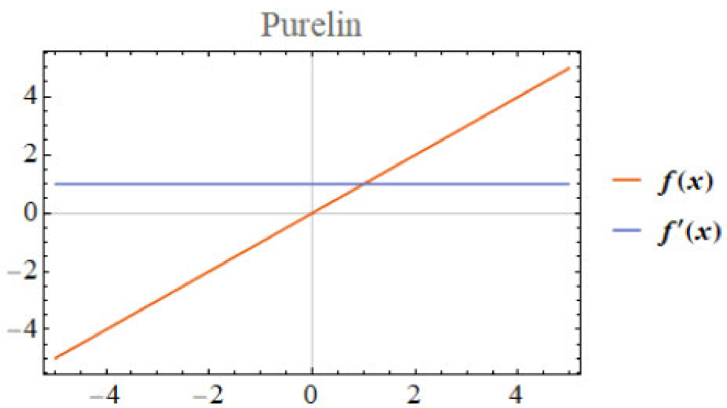

Figure 2.12: The Graph of Purlin Activation Function. *Source:* (Aldakheel, Satari, & Wriggers, 2021)

- **Nonlinear Activation Function:** This type of activation function is used to solve the complex nonlinearity relationship between the inputs and output data. Examples are the sigmoid activation function and Hyperbolic tangent activation function. They can be represented graphically and mathematically as:

  a. **Sigmoid activation function**

$$\boldsymbol{f(x) = \frac{1}{e^{-x}+1}\ ; \qquad f'(x) = \frac{e^{-x}}{(e^{-x}+1)^2}} \tag{2.11}$$

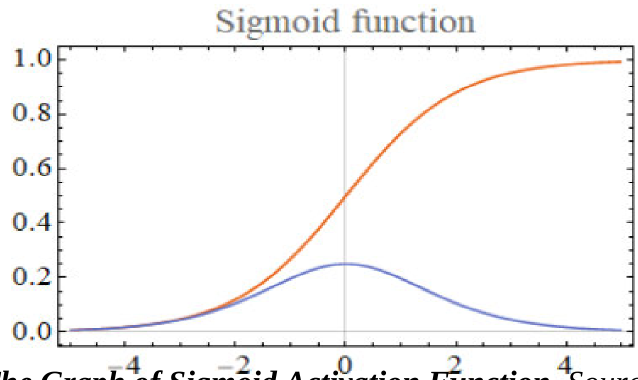

Figure 2.13: The Graph of Sigmoid Activation Function. Source: (Aldakheel, Satari, & Wriggers, 2021)

b. The hyperbolic tangent activation function

$$f(x) = \frac{e - e^{-x}}{e^{x} + e^{-x}}\ ;\quad f'(x) = 4\frac{e^{2x}}{(e^{2x} + 1)^{2}} \tag{2.12}$$

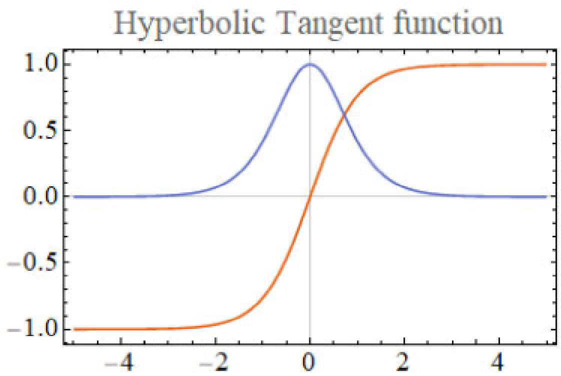

Figure 2.14: The Graph of* Hyperbolic Tangent *Activation Function. Source: (Aldakheel, Satari, & Wriggers, 2021)

2.13 ADVANTAGES OF COMPOSITE MATERIAL

Summary of the advantages exhibited by composite materials:

1. Composites have an extremely high stiffness or strength-to-weight ratio, which tends to improve performance while lowering energy consumption (Herakovich, Mechanics of Fibrous Composites, 1998). When compared to metals, composites can save up to 25% – 40% of weight (Blessley, 2002).
2. Composites outperform most metals in terms of corrosion, degradation, and fatigue resistance. Estimation of fatigue life is critical in aircraft, bridges, vehicles, and any

structure subjected to cyclic loading; thus, such structures are best designed with composite material. (Herakovich, Mechanics of Fibrous Composites, 1998).

3. Composites have consistent dimensions. This is because they have low thermal stress as a result of their low thermal expansion and conductivity (Blessley, 2002).
4. Most composites are non-conductors of electricity. This is an advantage as they reduce the possibility of electrocution and yet carry out the structural function of the metals.
5. Composites are formed efficiently with little or no material waste using an automated method which leads to a low cost of fabrication (Herakovich, Mechanics of Fibrous Composites, 1998).
6. Composites can withstand a twisting load. This implies high spinning speeds, fewer alternate bearings, and fewer supporting structural components. As a result, leads to a reduction in overall part count as well as production and design costs (Blessley, 2002).

2.14 LIMITATIONS OF COMPOSITE STRUCTURE

Summary of the limitations of composite materials (Marti'nez, 2008):

1. The raw materials needed in the manufacture of composites are expensive.
2. It is difficult to analyze composites.
3. Recycling and discarding composites are not easy because of how it was fabricated.
4. The matrix is deteriorating due to environmental factors.
5. Repair introduces new issues, such as materials that require refrigerated transport and storage and have a limited shelf life. Hot curing is required in many cases, necessitating special tooling, and hot or cold curing takes time.

2.15 APPLICATIONS OF COMPOSITE MATERIALS

Composites have found their applications in so many areas, starting from Stone Age. Presently, composites find their applications not only in engineering fields and industry (Marti'nez, 2008), but in all fields of study. The applications of composites can be summarized as;

1. Composites have found use in the automobile industry in the production of automobile parts such as motor engines, spray nozzles, mudguards, tires, and so on.
2. The aerospace industry is one of those that has benefited from the advancement of composite materials. This was due to the need for aircraft to be lightweight to improve performance and reduce fuel consumption. Composite materials are used in the construction of aircraft structural parts such as wings, bodies, and stabilizers, as well as aircraft engines (Marti'nez, 2008). Composite materials are also used in military rockets. Composite has also found its application in the maritime industry.
3. Shafts, hulls, spars, and other parts of ships are made of composite
4. In civil engineering, composite materials have been utilized in so many areas, especially in the areas of construction to prevent corrosion in reinforcements and reduce weights on a structure (Oller S. , Numerical Simulation of Mechanical Behavior of Composite Materials, 2014). Glass, aramid, and carbon fibre composites are increasingly being studied for pre-tensioning, post-tensioning, and reinforcing concrete. FRP systems may potentially be employed in concrete bridge decks or other outdoor concrete flooring structures to replace corroding steel rebars. Not only can 'pultruded' fibre reinforced plastic (FRP) sections replace steel in many load-bearing structures, but strengthening concrete beams with internally or externally bonded fibre-reinforced plastics (FRP) has also been shown to improve the load-bearing capacity and stiffness of existing structures (Hui & Dutta, 1998).
5. Sports have been improved with the growth of composite materials. Majorly, the lightweight of composite materials is what prompted the research of its application in

the sports field. Sports equipment where composites have been applied are; golf sticks, tennis rackets, pole shaft, hockey sticks (Zhang L. , 2015), etc.

6. Composites have also found their way into the communication sector. It is applied in the preparation of antenna and electronic circuit board.

In summary, this research tends to apply data-driven computational mechanics in solving for the properties and behaviours of the constituents of the composite material. This research provides an approach that combines data-driven computational homogenization, traditional computational homogenization, and contact mechanics. It fills a gap in the literature by providing a link that connects computational homogenization, contact mechanics and data-driven homogenization. Solving the RVE of the composite material using computational homogenization gave the database which was used for the data-driven multiscale analysis. Contact behavior between the constituents was calculated using the contact mechanics to know the debonding and displacement jump between the constituents.

CHAPTER 3

METHODOLOGY

3.1 INTRODUCTION TO MULTISCALE COMPUTATIONAL HOMOGENIZATION

To get a good macroscopic response of composite material, the base material should be enhanced by adding microscopic matter (Zohdi & Wriggers, 2005). Modern multiscale is one of the recent computational techniques for nonlinear simulations which uses scale transitions for solving problems in science and engineering (Geers M. G., Kouznetsova, Matouš, & Yvonnet, 2017).

Computational homogenization is a multiscale method that studies the nonlinear behaviour of a heterogeneous material using the knowledge of the finite element and the behaviour of the microstructure. It correlates the heterogeneous macroscopic structure with a homogeneous one using a suitably well-defined Representative Volume Element, RVE which has every inhomogeneity and non-linearity of the structure (Drosopoulos, Wriggers, & Stavroulakis, A multi-scale computational method including contact for the analysis of damage in composite materials, 2014). The RVE should at least pick out the inhomogeneity in the microscopic structure and should also be big enough to show how the heterogeneous material behaves (Fish & Yu, 2001). The Multiscale homogenization approach uses a unit cell, called, RVE which represents the entire subscale, of the microstructural subregion of a structure (Otero, Oller, Martinez, & Salomón, 2015).

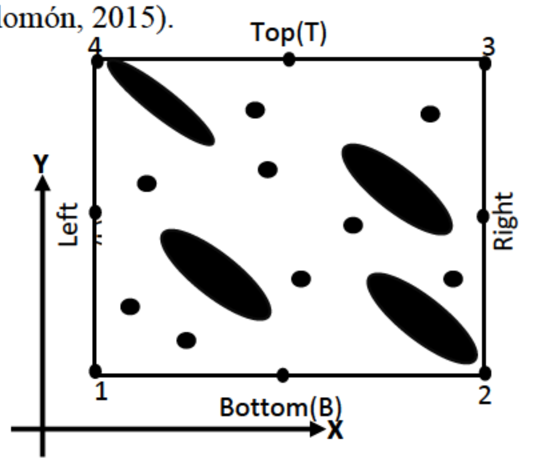

Figure 3.1; A 2D Representation of RVE Showing the Internal Nodes and Restrain Nodes: *source: (Okereke & Keates, 2018)*

An RVE is used to strictly model portions of the heterogeneous microstructure of a composite material layer (Hirschberger, Ricker, Steinmann, & Sukumar, 2009). Also, Otero et al, (Otero, Oller, Martinez, & Salomón, 2015) said that RVE determines the properties of the homogenized macroscale. The RVE portrays or depicts the microscopic nature of the whole heterogeneous composite structure. It is usually represented with a simple rectangular model. At every integration point in the macrostructure, the RVE is being called. The integration or gauss point is the point within an element in which numerical integration is evaluated

The RVE was loaded with a loading strain, $\boldsymbol{\varepsilon^M}$**,** called the macroscopic loading. This loading strain is used after simulation to calculate the homogenized stress**,** $\boldsymbol{\sigma^M}$**,** and the homogenized stiffness, $\boldsymbol{C^M}$**.** The three parameters are related as follows:

$$\boldsymbol{\sigma^M = C^M : \varepsilon^M} \tag{3.1}$$

To get the macroscopic stress and the tangent stiffness, the average relation between the micro and the macrostructure have to be obtained first by applying suitable boundary conditions.

3.2 RELATIONSHIP BETWEEN MICROSCOPIC AND MACROSCOPIC SCALE

The key difference between the macroscopic and microscopic scale of composite material is that the macroscopic scale deals with the simulation of the properties of composite material in bulk whereas the microscopic scale deals with the simulation of the properties of the constituents of the composite material.

The microscopic properties of the composite material are first solved, and the result from the microstructure is incorporated in the macrostructure to calculate the macroscopic properties of the composite material.

Formulation of the Microscopic Boundary Conditions

There are three major boundary conditions used that can be applied to the RVE;

- Prescribed linear displacement boundary condition
- Periodic boundary conditions.
- Prescribed tractions boundary conditions

For this research, the first two will be considered.

Prescribed Linear Displacement Boundary Condition

The prescribed linear displacement boundary condition is a common boundary condition. These are values which when applied to the nodes, displace them at a constant value. It is used

$$d_n|_{\partial V_\Omega} = \varepsilon^M x_n \quad \text{for n = 1, 2, …, n} \qquad \textbf{(3.2)}$$

to restrain all the nodes on the boundary of the RVE. The prescribed boundary condition is given by:

Where ε^M represents the loading strain,

∂V_Ω represents the boundaries of the RVE

x_n represents the boundary coordinates of the nodes of the RVE.

n represents the number of nodes.

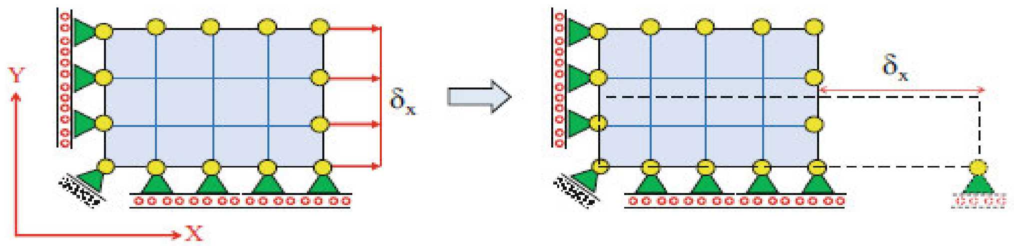

Figure 3.2: Prescribed Linear Displacement Boundary Condition on RVE and its Deformation Profile *source: (Okereke & Keates, 2018)*

Periodic Boundary Conditions

Periodic boundary conditions say that the opposite sides of the RVE after deformation should be a mirror reflection of each other. This means that the number of nodes on opposite sides must be equal (Okereke & Keates, 2018).

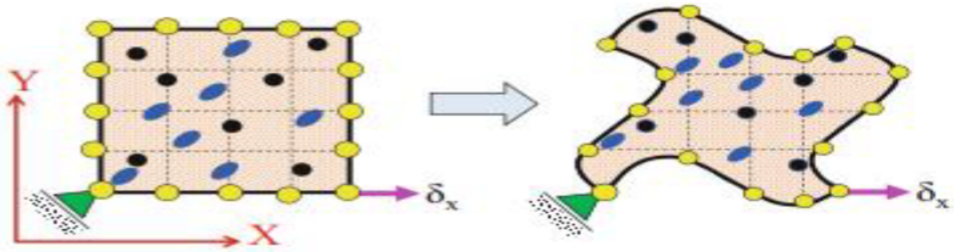

Figure 3.3: A typical Periodic Boundary Condition on RVE and its Deformation Profile
source: (Okereke & Keates, 2018)

There should be a connection between the displacement of the restrained nodes and the edge nodes. This connection is used when forcing an axial deformation, say $\boldsymbol{\delta_x}$.

To derive the periodic boundary conditions of the RVE shown in ***Fig 3.4***, we can make use of the ***canonical equation.*** A canonical equation is an equation whose Right-Hand Side (RHS) is always equal to zero.

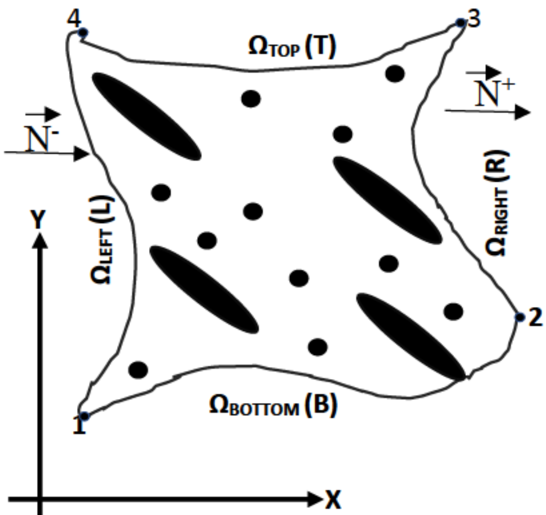

Figure 3.4: A 2D Illustration of an RVE: *Source: (Oller S. , Numerical Simulation of Mechanical Behavior of Composite Materials, 2014)*

Considering the internal (edge) nodes;

$$d_T = d_B; \qquad \textbf{(3.3a)}$$
$$\rightarrow d_T - d_B = 0$$

Also,

$$d_R = d_L;$$
$$\rightarrow d_R - d_L = 0 \qquad \textbf{(3.3b)}$$

Where d_T represents the displacement at the Top.

d_B represents the displacement at the Bottom.

d_R represents the displacement at the Right.

d_L represents the displacement at the Left

Considering the restrained (corner) nodes;

$$d_4 = d_1;$$
$$\rightarrow d_4 - d_1 = 0 \quad \textbf{(3.4a)}$$

Also,

$$d_2 = d_1;$$
$$\rightarrow d_2 - d_1 = 0 \quad \textbf{(3.4b)}$$

Where d_1 represents the displacement at the corner node 1,

d_2 represents the displacement at the corner node 2,

d_4 represents the displacement at the corner node 4,

Combining (3.3a) and (3.4a) gives;

$$(d_T - d_B) - (d_4 - d_1) = 0$$
$$\rightarrow (d_T - d_B) = (d_4 - d_1) \quad \textbf{(3.5a)}$$

Combining (3.3b) and (3.4b) gives;

$$(d_R - d_L) - (d_2 - d_1) = 0$$
$$\rightarrow (d_R - d_L) = (d_2 - d_1) \quad \textbf{(3.5b)}$$

Therefore, the periodic boundary condition is given by (3.6);

$$(d_T - d_B) = (d_4 - d_1) \quad \textbf{(3.6a)}$$
$$(d_R - d_L) = (d_2 - d_1) \quad \textbf{(3.6b)}$$

3.3 HOMOGENIZATION SCHEME

Firstly, the averaging relation for both stress and strain will be the first thing to get. The energy averaging theorem by R. Hill, (Hill, 1963) is a commonly averaging theorem used to relate macroscopic and microscopic problems. It says that the volume average macroscopic strain

$$\boldsymbol{\varepsilon^M = \frac{1}{V_\Omega} \int_{V\Omega} \varepsilon^m dV_\Omega} \quad \textbf{(3.7)}$$

tensor, $\boldsymbol{\varepsilon^M}$,equals the average volume of the microscopic strain tensor, $\boldsymbol{\varepsilon^m}$. The homogenization scheme in this work follows the pattern of (Drosopoulos, Wriggers, & Stavroulakis, A multi-scale computational method including contact for the analysis of damage in composite materials, 2014), (Verhaegh, 2020) and (Miehe & Koch, 2002).

Where V_Ω represents the average volume of the RVE and the microscopic strain can be related to displacement using:

Where $\boldsymbol{\nabla}$ represents the gradient operator in the microscopic scale

$\boldsymbol{d^m}$ represents the displacement in the microscopic scale

$$\boldsymbol{\varepsilon^m = \frac{1}{2}[\nabla d^m + (\nabla d^m)^T]} \quad \textbf{(3.8)}$$

$$\boldsymbol{\varepsilon^M = \frac{1}{V_\Omega}\int_{V\Omega} \frac{1}{2}[\nabla d^m + (\nabla d^m)^T] dV_\Omega} \quad \textbf{(3.9)}$$

Substituting (3.8) in (3.7) helps to relate microscopic displacement to the macroscopic strain.

The averaging theorem for stress says that the volume average macroscopic stress tensor, $\boldsymbol{\sigma^M}$, equals the average volume of the microscopic stress tensor, $\boldsymbol{\sigma^m}$.

$$\boldsymbol{\sigma^M = \frac{1}{V_\Omega}\int_{V\Omega} \sigma^m dV_\Omega} \quad \textbf{(3.10)}$$

Equation (3.7) can be solved by integration, and the solution says that the loading or macroscopic strain on the boundaries of the RVE equals the volume average of the microscopic strain, shown thus:

$$\boldsymbol{\varepsilon^M = \varepsilon^m} \quad \textbf{(3.11)}$$

Equation (3.9) can be solved in two ways. It can be solved considering the prescribed linear boundary condition on the RVE or by considering periodic boundary conditions on the RVE. According to (Drosopoulos, Wriggers, & Stavroulakis, A multi-scale computational method including contact for the analysis of damage in composite materials, 2014), (Miehe & Koch, 2002), the application of prescribed linear boundary condition on the RVE gives the solution of (3.9) as:

$$\boldsymbol{\sigma^M} = \boldsymbol{\sigma^m} = \frac{\mathbf{1}}{\boldsymbol{V_\Omega}} \boldsymbol{fX} \quad \textbf{(3.12)}$$

Where σ^m represents the microscopic stress,

$\boldsymbol{f}$ represents the matrix of external forces on the edge of the RVE

$\boldsymbol{X}$ represents the undeformed coordinates of the nodes at the boundary of the RVE.

(Drosopoulos, Wriggers, & Stavroulakis, A multi-scale computational method including contact for the analysis of damage in composite materials, 2014), (Miehe & Koch, 2002) gave the solution of equation (3.9), if periodic boundary condition was applied on the RVE as follows;

$$\boldsymbol{\sigma^M} = \boldsymbol{\sigma^m} = \frac{\mathbf{1}}{\boldsymbol{V_\Omega}} \boldsymbol{f}^* \boldsymbol{X}^* \quad \textbf{(3.13)}$$

Where $\boldsymbol{f}^*$ represents the external forces as a result of prescribed displacements on the three corner nodes of the RVE and X^* represents the undeformed coordinates of the three corner nodes.

Steps Involved in the Formulation of the Homogenization Scheme

In this part, the steps involved in the homogenization of the microscopic RVE are presented. The formulation followed here is the same as that followed in (Drosopoulos, Wriggers, & Stavroulakis, A multi-scale computational method including contact for the analysis of damage in composite materials, 2014), (Verhaegh, 2020), and (Miehe & Koch, 2002), for both prescribed linear displacement and the periodic boundary conditions on the RVE.

3.4 BOUNDARY CONDITION

For Prescribed Linear Displacements Boundary Condition;

In prescribed linear displacements, the system of equations involved is partitioned into restrained (*r*) and free (*f*) degrees of freedom after convergence.

$$\begin{bmatrix} K_{rr} & K_{rf} \\ K_{fr} & K_{ff} \end{bmatrix} \begin{bmatrix} d_r \\ d_f \end{bmatrix} = \begin{bmatrix} f_r \\ 0 \end{bmatrix} \quad \textbf{(3.13)}$$

Where, K_{rr} represents the boundary condition in the node restrained both in x and y axes

K_{ff} represents the boundary condition in the node free both in x and y axes

K_{fr} represents the boundary condition in the node free in x-axis and restrained in y-axis

K_{rf} represents the boundary condition in the node free in y-axis and restrained in x-axis

Equation (3.13) can be simplified further to get K_M by eliminating the free degree of freedom. The result of the simplification is shown as;

$$K_M d_r = f_r \tag{3.14}$$

$$K_M = K_{rr} - K_{rf} K_{ff}^{-1} K_{fr} \tag{3.15}$$

For Periodic Boundary Condition

Following the procedures in (Drosopoulos, Wriggers, & Stavroulakis, A multi-scale computational method including contact for the analysis of damage in composite materials, 2014), considering (3.6), and transformation of the systems of equations, the system of equations involved is partitioned into unconstrained (u) and constrained (c) degrees of freedom:

$$C\delta d = 0$$

$$\rightarrow [C_r \;\; C_c] \begin{bmatrix} \delta d_r \\ \delta d_c \end{bmatrix} = 0 \tag{3.16}$$

Equation (3.16) can be simplified further to give:

$$d_c = C_{rc} d_r \tag{3.17}$$

$$C_{rc} = -C_c^{-1} C_r \tag{3.18}$$

Recall that,

$$f^p = r_u + C_{cu}^T r_c \tag{3.19}$$

$$K^p d_u = f^p \tag{3.20}$$

$$K^p = K_{uu} - K_{uc} C_{uc} + C_{uc}^T K_{cu} + C_{cu}^T K_{cc} C_{cu} \tag{3.21}$$

Substituting equations (3.19) and (3.21) into equation (3.20) and transforming the above system of equations into a condensed system of equations gives:

$$d_u(K_{uu} + C_{uc}^T K_{cu} + K_{uc} C_{uc} + C_{uc}^T K_{cc} C_{cu}) = r_u + C_{cu}^T r_c \quad \textbf{(3.22)}$$

Equation (3.22) can be solved by partitioning it into restrained (r) and free (f) degrees of freedom:

$$\begin{bmatrix} K_{rr}^p & K_{rf}^p \\ K_{fr}^p & K_{ff}^p \end{bmatrix} \begin{bmatrix} d_r \\ d_f \end{bmatrix} = \begin{bmatrix} f_r^p \\ 0 \end{bmatrix} \quad \textbf{(3.23)}$$

Equation (3.23) can be simplified further to get the reduced matrix, K_M^p by eliminating the free degree of freedom. The result of the simplification is;

$$K_M^p\, d_r = f_r^p \quad \textbf{(3.24)}$$

$$K_M^p = K_{rr}^p - K_{rf}^p K_{ff}^{p\,-1} K_{fr}^p \quad \textbf{(3.26)}$$

Getting the Consistent Stiffness Matrix

The consistency stiffness matrix can be calculated at every integration point, by formulating the relationship between stress and strain in the macroscopic structure. Both periodic boundary conditions and prescribed linear displacement boundary conditions can be used for the calculation of the consistency tangent stiffness. But for this research, I chose to use periodic boundary conditions. When periodic boundary conditions are applied to the three corner nodes of the RVE, the displacement due to the loading strain is given by;

$$d_r = M_u \varepsilon^M \quad \textbf{(3.27)}$$

Where ε^M represents the loading strain

M_u represents the matrix of the undeformed nodal coordinates of the RVE.

Recall that the stress on the RVE from the averaging theorem is equivalent to the stress on the macroscopic structure and can be gotten from the relation:

$$\sigma^m = \sigma^M = \frac{1}{V_\Omega} M_u^T f_r^p \quad \textbf{(3.28)}$$

Where f_r^p represents the external force on the three corner nodes of the RVE

The consistent tangent stiffness matrix, C^M which relates stress and strain at the macroscopic level can be calculated by substituting equations (3.24) and (3.27) in equation (3.28).

$$\sigma^M = \frac{1}{V_\Omega} M_u^T (K_M^p (M_u \varepsilon^M)) \tag{3.29}$$

Rearranging equation (3.29) gives;

$$\sigma^M = \frac{1}{V_\Omega} M_u M_u^T K_M^p \varepsilon^M \tag{3.30}$$

From the relation in equation (3.30), it shows that;

$$C^M = \frac{1}{V_\Omega} M_u M_u^T K_M^p \tag{3.31}$$

The equation (3.31) gives the relation which can be used to calculate the value of the tangent stiffness matrix.

3.5 CONTACT BETWEEN MATRIX AND FIBRES OF COMPOSITE STRUCTURE

A small change in geometry is assumed while applying finite elements to contact problems of two discretized bodies so that purely nodal basis and general linear theory can be applied (Wriggers P. , 2006)

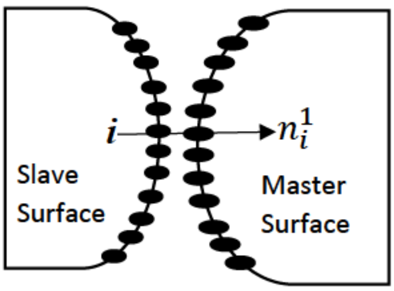

Figure3.5: Nodal discretization for Matrix-Fibre Interface Used in MATLAB:
Source: (Drosopoulos, Wriggers, & Stavroulakis, A multi-scale computational method including contact for the analysis of damage in composite materials, 2014)

To study the interaction between the fibre and the matrix, the unilateral contact law for pair of nodes, ***i***, shown in ***Figure3.5*** is used, following the relation in (Drosopoulos, Wriggers, &

Stavroulakis, A multi-scale computational method including contact for the analysis of damage in composite materials, 2014), (Wriggers P. , 2006), (Georgiadis, Stavroulak, Koltsakis, & Panagiotopoulos, 1990). The relation is shown as:

$$g_{Ni} = \left(d_i^2 - d_i^1\right).n_i^1 + \beta_i \geq 0 \quad \textbf{(3.32a}$$

$$t_{Ni} \leq 0 \quad \textbf{(3.32b)}$$

$$g_{Ni} t_{Ni} = 0 \quad \textbf{(3.32c)}$$

Where g_{Ni} represents the gap between the two surfaces in contact.

d_i^2 *and* d_i^1 represents the displacement of each node in the interface, ***i***

n_i^1 represents a unit normal vector to the master surface

β_i represents a potential initial gap which is usually zero for perfectly bonded constituents.

Inequality (3.32a) says that there is no penetration between the two surfaces

Inequality (3.32b) says that tensile stress is not allowed in the interface

Equation (3.32c) says that at the interface, there is contact with tensile stress or there is no contact without tension stress.

Calculation of the unit normal vectors to the master's surface is calculated, followed by writing relations in (3.32) for the whole structure. Then, a MATLAB code is written to perform the above formulations (Drosopoulos, Wriggers, & Stavroulakis, A multi-scale computational method including contact for the analysis of damage in composite materials, 2014).

Lagrange Multiplier Formulation

The interaction between the constituents of the composite material at the microscopic level is studied in this section. To explore this, a Lagrangian formulation was integrated into the MATLAB code used for simulating the multiscale homogenization scheme. Another important tool integrated into the MATLAB code is the Newton-Raphson Iteration method which was used to calculate the behaviour of the constituents which are in contact in the microstructure of the composite material. The formulation of the Lagrange multiplier follows the formulations in (Wriggers P. , 2006).

Applying Lagrange multiplication to (3.32) gives;

$$\int_{\Omega_c} \delta\lambda_N \, g_N d\Omega \;\rightarrow\; \sum_{i=1}^{n_c} \delta\lambda_{Ni} \, g_{Ni} A_i = \sum_{i=1}^{n_c} \delta\lambda_{Ni} \, [(d_i^2 - d_i^1).n_i^1 + \beta_i] A_i \tag{3.33}$$

The relation (3.32a) can be reformed into (3.34) if the initial gap is independent of the displacement field.

$$\delta g_{Ni} = \left(\eta_i^2 - \eta_i^1\right).n_i^1 \tag{3.34}$$

Applying LAGRANGE multiplication to (3.34) gives;

$$\int_{\Omega_c} \lambda_N \, \delta g_N d\Omega \;\rightarrow\; \sum_{i=1}^{n_c} \lambda_{Ni} \, \delta g_{Ni} A_i = \sum_{i=1}^{n_c} \lambda_{Ni} \left(\eta_i^2 - \eta_i^1\right).n_i^1 A_i \tag{3.35}$$

Where n_c represents the active contact nodes

$\eta_i^2 - \eta_i^1$ represents the test function

λ_{Ni} represents the Lagrange multiplier at node ***i*.**

$\lambda_{Ni} A_i$ represents the nodal force related to node ***i*.**

We can introduce two vectors at node ***i***, to obtain the discretized form of (3.33) and (3.35). The vectors are;

$$\Delta\hat{d}_i = \begin{Bmatrix} \Delta d_i \\ \Delta\lambda_i \end{Bmatrix} \text{ and } \quad \hat{\eta}_i = \begin{Bmatrix} \eta_i \\ \delta\lambda_i \end{Bmatrix} \tag{3.36a}$$

With,

$$\Delta d_i = \begin{Bmatrix} \Delta d_i^2 \\ \Delta d_i^1 \end{Bmatrix} \text{ and } \quad \eta_i = \begin{Bmatrix} \eta_i^2 \\ \eta_i^1 \end{Bmatrix} \tag{3.36b}$$

Substituting (3.36) in (3.33) and (3.35);

$$\int_{\Omega_c} (\delta\lambda_N \, g_N + g_N \delta) d\Omega \approx \sum_{i=1}^{n_c} \hat{\eta}_i{}^T \, G_i^{cL} \tag{3.37}$$

Where,

$$G_i^{cL} = \begin{Bmatrix} \lambda_{Ni} C_i \\ d_i^T C_i \end{Bmatrix} A_i \tag{3.38}$$

$$C_i = \begin{Bmatrix} n_i^1 \\ -n_i^1 \end{Bmatrix} \tag{3.39}$$

$$d_i = \begin{Bmatrix} d_i^2 \\ d_i^1 \end{Bmatrix} \tag{3.40}$$

Further simplification (3.37), by linearization, gives;

$$\hat{\eta}_i \; K_i^{cL} \; \Delta \hat{d}_i;$$

$$K_i^{cL} = \begin{bmatrix} 0 & C_i \\ C_i^T & 0 \end{bmatrix} A_i \tag{3.41}$$

Where K_i^{cL} represents the contact stiffness matrix for node ***i.***

After getting the Lagrangian formulations, the next thing is to minimize the potential energy of the system (Georgiadis, Stavroulak, Koltsakis, & Panagiotopoulos, 1990). This is done by selecting an optimized method that shows the equilibrium system and contact restraints of the constituents of the composite material in the microstructure (Drosopoulos, Wriggers, & Stavroulakis, A multi-scale computational method including contact for the analysis of damage in composite materials, 2014). The approach of (Drosopoulos, Giannis, Stavroulaki, & Stavroulakis, 2018) and (Georgiadis, Stavroulak, Koltsakis, & Panagiotopoulos, 1990) was followed;

$$minimize\left(\prod = \frac{1}{2}\, d^T K d - P^T d\right) \tag{3.42a}$$

$$g_N = Cd - \beta \geq 0 \tag{3.42b}$$

$$t_N \leq 0 \tag{3.42c}$$

Where g_N represents the gap function

t_N represents normal forces in the interface of contact

P^T represents the external loading vector

β represent a potential initial gap that is usually zero for perfectly bonded constituents.

Equation (3.42a) represents the function of the equilibrium of the system.

Inequality (3.42b) says that there is no penetration between the two surfaces.

Inequality (3.42c) says that tensile stresses are not allowed in the interface.

The inequalities (3.42b) and (3.42c) can be optimized by introduction of penalty method as follows;

$$\nabla \prod + \frac{1}{2} \epsilon_N \nabla g_N^T g_N + \nabla \lambda_N^T g_N \quad \textbf{(3.43)}$$

Substituting (3.42) into (3.42), the equilibrium equation changes to;

$$F(u) = 0\ ;$$
$$Kd - P + \lambda_N^T C + \epsilon_N C^T C d - \epsilon_N C^T \beta = 0 \quad \textbf{(3.44)}$$

Equation (3.44) can be linearized by the use of Newton-Raphson's Iterative method as thus;

$$(K + \epsilon_N C^T C)\delta d = -(Kd - P + \lambda_N^T C + \epsilon_N C^T C d - \epsilon_N C^T \beta) \quad \textbf{(3.45)}$$

Which can be written as;

$$C^m \delta d = -\boldsymbol{R}; \quad (3.46)$$

But

$$C^m = K + \epsilon_N C^T C \quad (3.47)$$

Where **R** represents the residual force offered by nodes in contact

C^m represents RVE tangent stiffness matrix

K represents the initial RVE stiffness matrix

ϵ_N represents the penalty constant

The last step involved after integrating contact mechanism and Augmented Lagrangian formulation into multiscale analysis is the calculation of the macroscopic tangent stiffness matrix and the macroscopic stress.

Firstly, the RVE stiffness tangent, C^m is calculated at every gauss point after convergence by partitioning equation (3.47). After calculating C^m, the next thing is to apply the boundary condition. If the prescribed linear displacement boundary condition is applied, equation (3.15) can be used for calculating the K_M, while equation (3.26) is used to calculate K_M^p if periodic boundary condition is applied. Then, the macroscopic stiffness tangent, C^M can be calculated using equation (3.31) and the macroscopic stress, σ^M, with equation (3.28).

3.6 DATA-DRIVEN MULTISCALE COMPUTATIONAL HOMOGENIZATION OF COMPOSITE STRUCTURE

Data Generation

A MATLAB code is developed for the analysis and convergence of a nonlinear finite element model of the representative volume element, RVE at every gauss point (Drosopoulos, Wriggers, & Stavroulakis, A multi-scale computational method including contact for the analysis of damage in composite materials, 2014). This simulation follows the homogenization scheme shown in the section above.

It involves the calculation of the microscopic stress and microscopic stiffness of the RVE at every gauss point. At every gauss point, the RVE is loaded with the macroscopic strain, $\boldsymbol{\varepsilon}^{\boldsymbol{M}}$, whose size is a 3X1 matrix, which after convergence gives the stress $\boldsymbol{\sigma}^{\boldsymbol{M}}$, whose size is a 3X1 matrix and tangent stiffness, $\boldsymbol{C^M}$, whose size is a 3X3 matrix. This procedure is repeated several times, depending on the strain loading.

After the convergence of the whole structure, two databases were created; a strain-stress database and a strain-stiffness database. The size of each database is 9621. The size was calculated using the formula:

$$\left\{\frac{|\varepsilon_{min}^{M}| + |\varepsilon_{max}^{M}|}{load\ step} + 1\right\}^{3} \qquad (3.48)$$

Where ε_{min}^{M} represents the minimum strain loaded = -1

ε_{max}^{M} represents the maximum strain loaded = 1

$load\ step$ represents the range of application = 0.1

In the strain-stress database, each strain is assigned to particular stress and in the strain-tangent stiffness database, each strain is also corresponding to a particular tangent stiffness.

Training Process

The two databases after being created were used to train two neural networks. The training is done with MATLAB, using a feed-forward backpropagation neural network. The diagrammatic representation of the feed-forward backpropagation Neural Network that is used for training the database is represented in ***Figure 3.6***

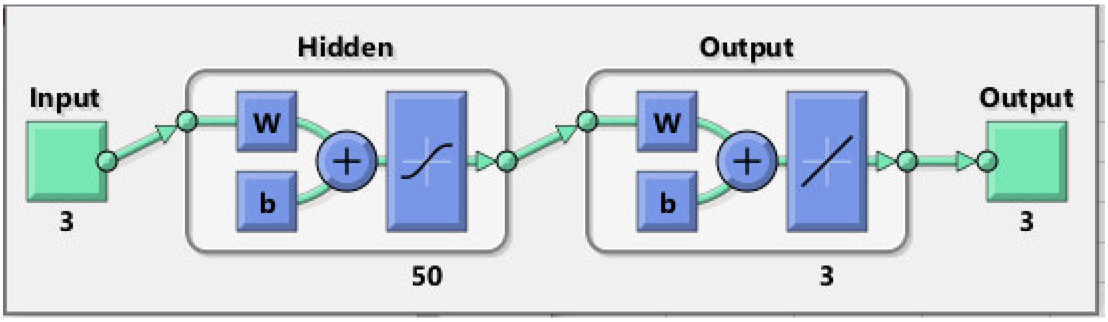

Figure 3.6: Diagrammatic Representation of the Neural Network for Training the Databases

The neural network consists of

- an input,
- one hidden layer of 50 neurons and
- an output layer with 3 neurons (strain-stress database)
- 80% of the data sample is used for training, 10% used for validation, and 10% for testing

In the course of training, the strain-stress database has strain as the input while stress is the target and, in the strain-tangent stiffness database, the strain is the input while tangent stiffness is the target. To train the neural network, half of the strain-stress database and half of the strain-stiffness database was used. The selection for the training of databases was done line by line, such that after selecting a line for training, the next line is skipped to the one after, till the end of the database. The other half was used to check for the accuracy of the Neural Network training.

Data-Driven Process

After the training has been concluded, the trained databases are used for a data-driven multiscale homogenization scheme which was run by MATLAB code.

According to ***Figure 3.6,*** the heterogeneous macroscopic structure is firstly represented by a homogeneous model. There was no assumption on the material properties of the homogeneous model, rather the mechanical characteristics are gotten using the multiscale analysis shown in the previous section. From ***Figure3.6,*** it can also be seen that at every gauss point in the homogeneous model that the strain, $\boldsymbol{\varepsilon^M}$, as an input calls the stress, $\boldsymbol{\sigma^M}$, and the tangent stiffness $\boldsymbol{C^M}$, as the outputs of the trained strain-stress and strain-tangent stiffness databases respectively.

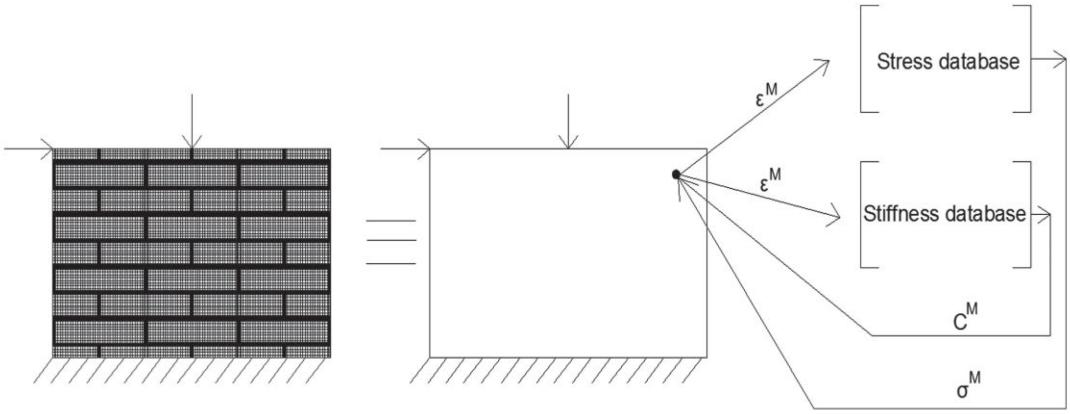

Figure 3.7: Data-Driven Multiscale Computational Homogenization of Composite Structure. *Source:* (Drosopoulos, Giannis, Stavroulaki, & Stavroulakis, 2018)

These outputs are then returned to the homogeneous model and the Newton-Raphson iterative method is used for the nonlinear material behaviour that was built numerically. The Newton-Raphson that was adopted is:

$$C^M(d_i)\delta d_{1+i} = -R(d_i) \tag{3.48}$$

Where;

$$R(d_i) = \int_V B^T \sigma(d_i)\, dV - F \tag{3.49}$$

$$C^M(d_i) = \frac{\partial R(d_i)}{\partial d} = \int_V B^T \frac{\partial \sigma(d_i)}{\partial d} dV \tag{3.50}$$

$$\rightarrow C^M(d_i) = \int_V B^T \frac{\partial \sigma(d_i)}{\partial \varepsilon} \frac{\partial \varepsilon}{\partial d} dV = \int_V B^T \frac{\partial \sigma(d_i)}{\partial \varepsilon} B dV \tag{3.51}$$

$$\therefore C^M(d_i) = \int_V B^T\, C^m B dV \tag{3.52}$$

Where F represents the external force vector.

C^M represents the macroscopic tangent stiffness matrix.

C^m represents the microscopic consistent stiffness matrix at each gauss point.

B represents the strain displacement matrix.

At every gauss point, Newton-Raphson's iteration method is used to calculate the consistent stiffness, C^m, and the stress, σ^m, by calling the two trained databases. Once the consistent stiffness and the stress are calculated, the tangent stiffness and the residual force can be calculated using equations (3.31) and (3.49) respectively.

CHAPTER 4

RESULTS AND DISCUSSION

In the course of this research, computation and simulation are done with MATLAB. A MATLAB code was developed to analyze and solve the stress and stiffness of the Representative Volume Element (RVE). The solution from the RVE gave the two databases; strain-stress and strain-stiffness database which was used for the data-driven homogenization process.

4.1 EFFICIENCY OF NEURAL NETWORK TRAINING

A feed-forward backpropagation Neural Network (NN) was used to train both databases and the predicted results are plotted with the result from the database to check for the efficiency of the NN.

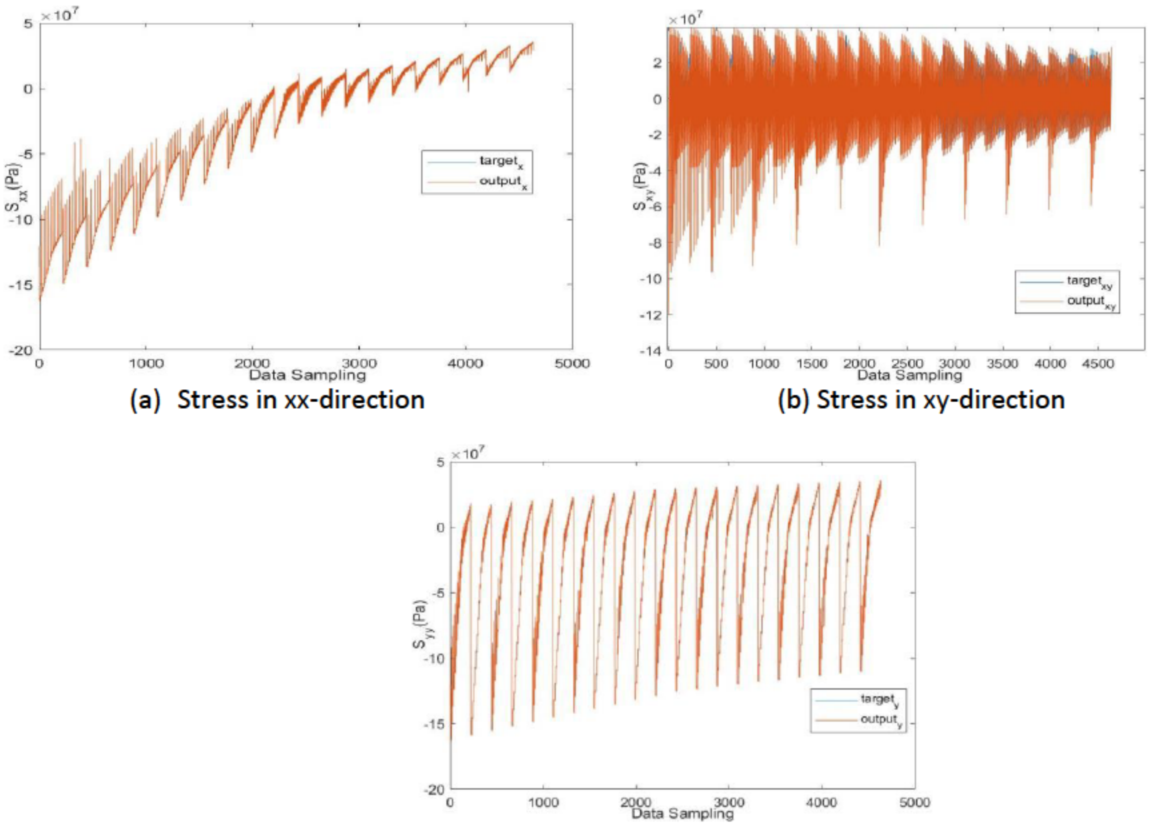

(a) Stress in xx-direction

(b) Stress in xy-direction

(c) Stress in yy-direction

Figure 4.1 Verification of the Stress Predicted by the NN in x-x, x-y, and y-y Directions

The result of the stress comparison is plotted as shown in ***Figure 4.1.*** The disparity between the target (stress from the database) and the output (stress) is minuscule, indicating that the prediction of the Neural Network is nice.

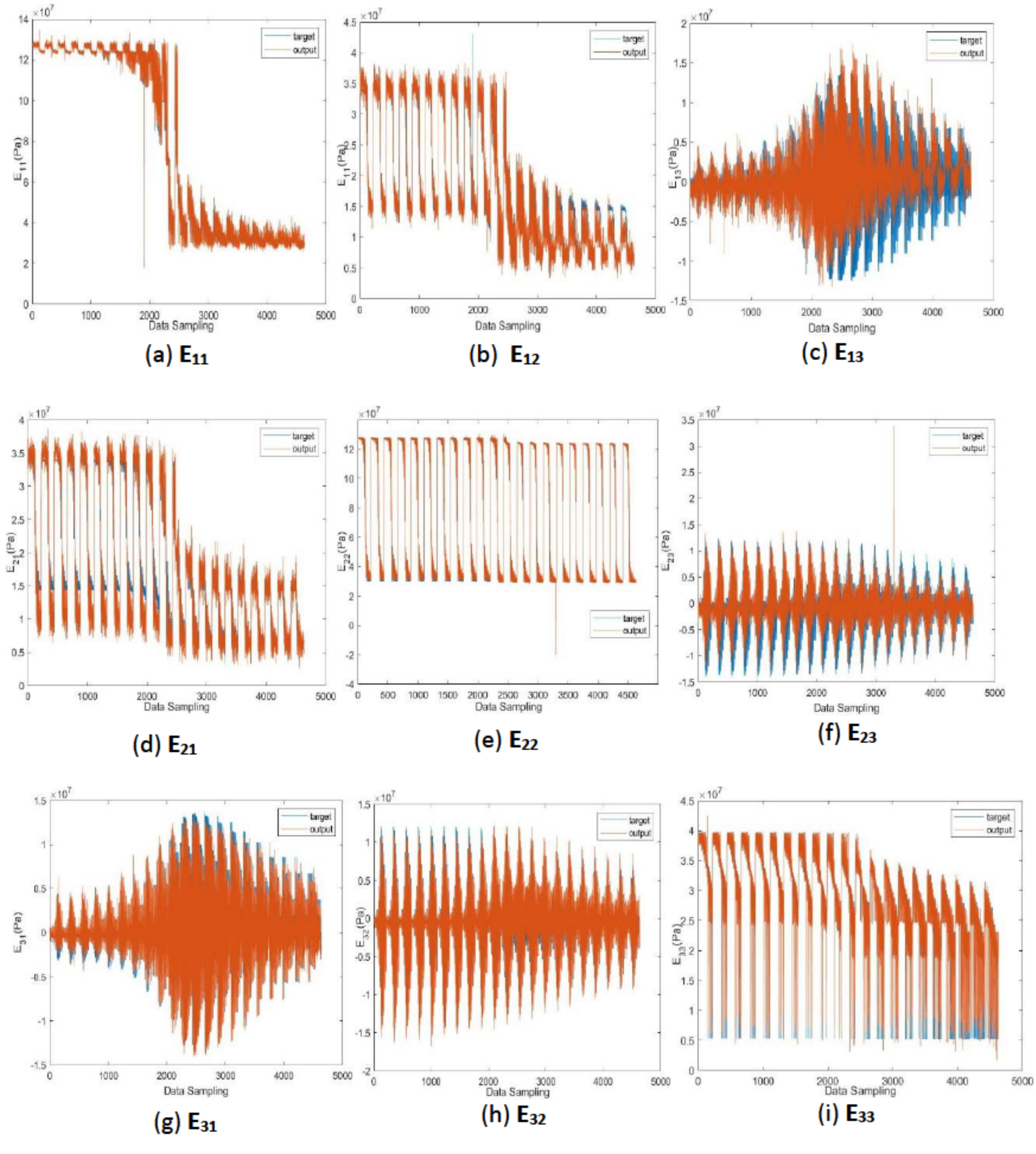

Figure 4.2 Verification of the Stiffness Predicted by the NN from **E_{11} to E_{33}**

Comparison between the NN predicted stiffness (output) and database stiffness (target) is shown in ***Figure 4.2***. From the graphs, it shows that the NN showed a satisfactory prediction but some part of the diagrams like those shown in ***Figure 4.2 (c), (f), (g)*** is less accurate. The less accuracy in some parts of the graph is not a problem because using the data-driven method, the multi-scale simulation obtains a new stiffness at each iteration whenever the NN is called.

4.2 MULTI-SCALE SCHEME.

After training, the results from the training are incorporated into the Macro-scale. This is done by calling the MATLAB code into a Multi-scale Macro-Increment code. The MATLAB code used in training the Neural Network is shown as:

```
function[y] = trainnn(strain)
% Solve an Input-Output Fitting problem with a Neural Network
% Script generated by Neural Fitting app
% Created 27-Jul-2021 12:19:07
%
% This script assumes these variables are defined:
%
%   strainn - input data.
%   elasticity - target data.
strainn = load('strainn.csv');
elasticity = load('elasticity1.csv');
x = strainn;
t = elasticity;

% Choose a Training Function
trainFcn = 'trainlm';  % Levenberg-Marquardt backpropagation.

% Create a Fitting Network
hiddenLayerSize = 50;
net = fitnet(hiddenLayerSize,trainFcn);

% Setup Division of Data for Training, Validation, Testing
net.divideParam.trainRatio = 80/100;
net.divideParam.valRatio = 10/100;
net.divideParam.testRatio = 10/100;

% Train the Network
[net,tr] = train(net,x,t);

% Test the Network
y = net(x);
e = gsubtract(t,y);
performance = perform(net,t,y)

% View the Network
view(net)

% Plots

figure, plotperform(tr);
figure, plottrainstate(tr);
figure, ploterrhist(e);
figure, plotregression(t,y);
figure, plotfit(net,x,t);
end
```

Figure 4.3: The MATLAB code used in training the Neural Network

A macroscopic structure to be considered is one microfibre whose mesh size is 25 elements as shown in ***Figure 4.4***.

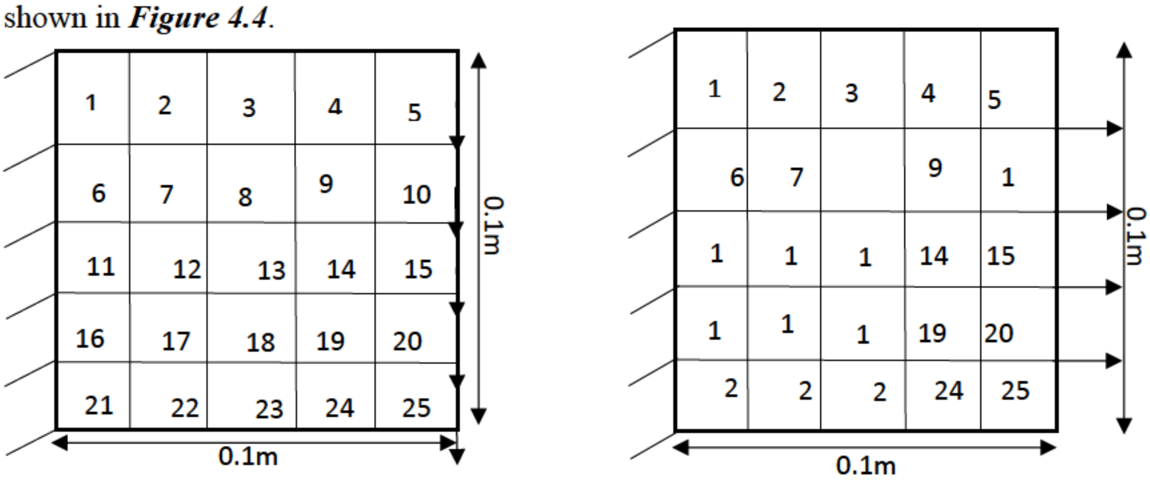

(a) Vertical Loading Condition (b) Horizontal Loading Condition

Figure 4.4: Macro Model of size 25 Elements with the Loading Condition.

After calling the Neural Network into a Multi-scale Macro-Increment MATLAB Code, the code calculated the following properties of the composite:

- Force displacement relationship
- Force debonding relationship
- Deformation of the macrostructure

Force Displacement Relationship:

When the structure was loaded as shown in ***Figure 4.4(a),*** the force-displacement diagram is shown in ***Figure 4.5.***

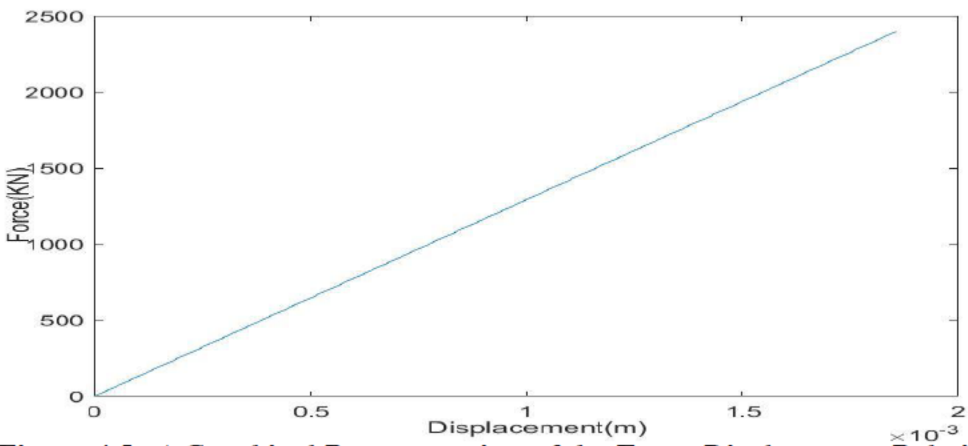

Figure 4.5: A Graphical Representation of the Force-Displacement Relationship.

The ***Force-Displacement Relationship*** shown in ***Figure 4.5,*** is a linear graph with a positive slope. It can be inferred that an increment in the force applied leads to an increase in the displacement by the composite.

To know the effect of mesh size on the macrostructure, the graph of force against displacement was plotted for a macro model whose mesh size is 16 macro elements, 25 macro elements, and 100 macro elements on the same axis. The graph is shown in ***Figure 4.6.***

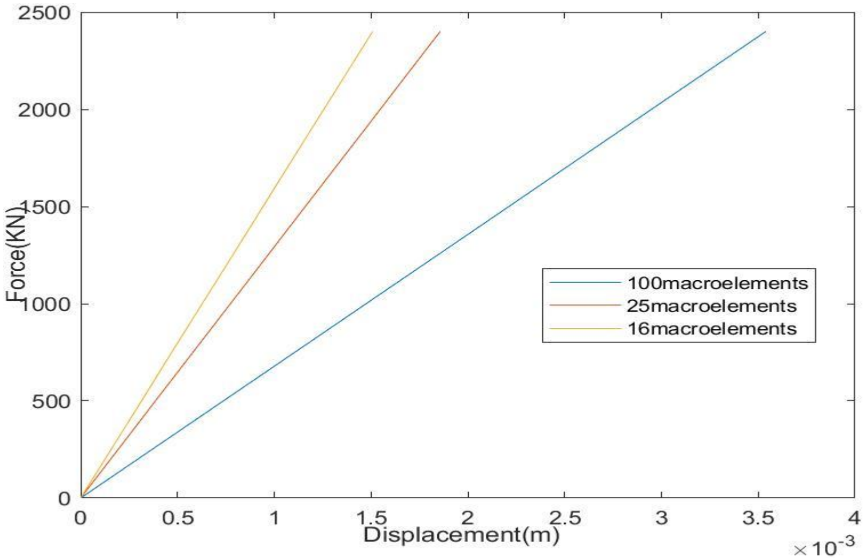

Figure4.6 A Force-Displacement Relationship for Different Mesh Sizes

From ***Figure 4.6***, it can be deduced that there is a gap between the graphs, which shows that mesh size influences the response of the macrostructure. From the figure, it is shown that the macrostructure with 100macro elements mesh will experience the highest displacement when the same forces are applied to all three macrostructures. The 25macro elements mesh size is used in this research for convenience.

The Force-displacement diagram of a composite structure tends to change when the direction of the macro loading is changed. It tends to change from linear to nonlinear. To investigate this, the loading condition in ***Figure 4.7*** is adopted. The loading condition in ***Figure 4.7(a)*** is a compressive load and causes no change in the interface of the constituents of the composite while that in ***Figure 4.7(b)*** is tensile and causes a gap between the constituents of this composite.

After simulation, the result is a non-linear graph shown in ***Figure 4.8.*** The interpretation shows that a change in the loading direction of the load affects the contact state in the interface of the composite.

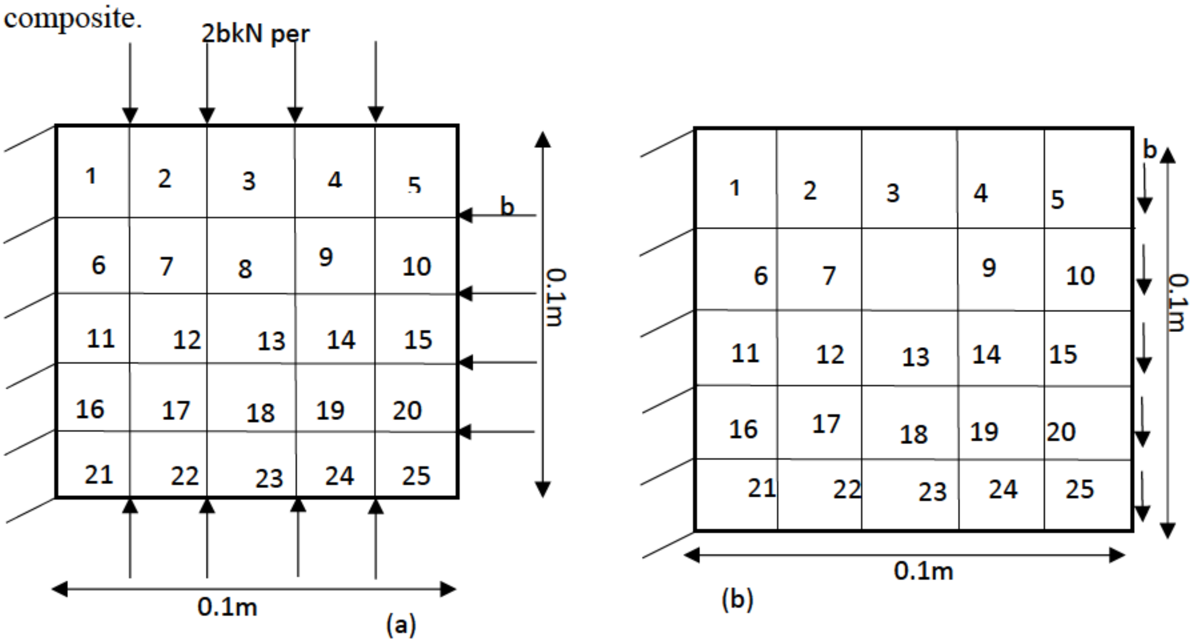

Figure 4.7: Investigation of Change in Direction of Macro Load on the Macrostructural Behaviour

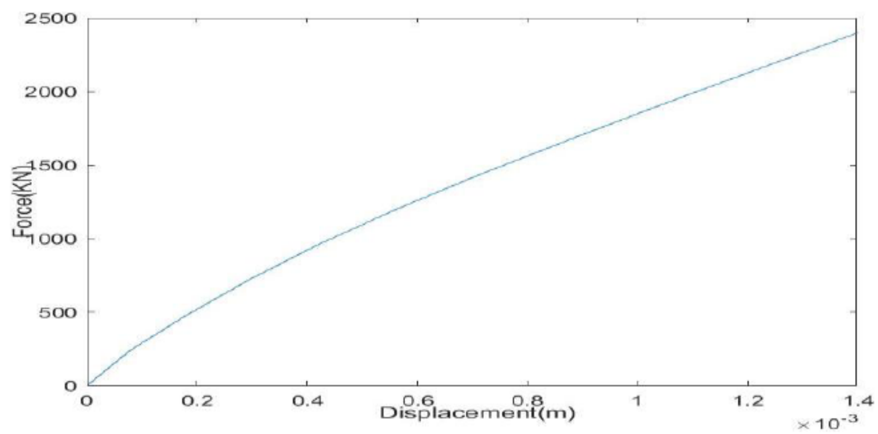

Figure 4.8: Force–Displacement Diagrams of The Macroscopic Structure for a Combined Loading

Force-Debonding Relationship

When there is a displacement jump amongst the constituents of macrostructure, as a result of an applied load on the structure, it leads to debonding. This multiscale approach calculates the debonding for each RVE at the corresponding gauss point on the macrostructure. This is the advantage of the Multiscale approach used here. The graph of force against debonding for the three most affected elements was plotted in ***Figure 4.9***.

When debonding occurs in a composite structure, it reduces the stiffness of the structure. The graph of force against debonding shows the region (Element) that suffers the most debonding. From the graph presented in ***Figure 4.9***, the section that suffers the major debonding is **$Element_1$.**

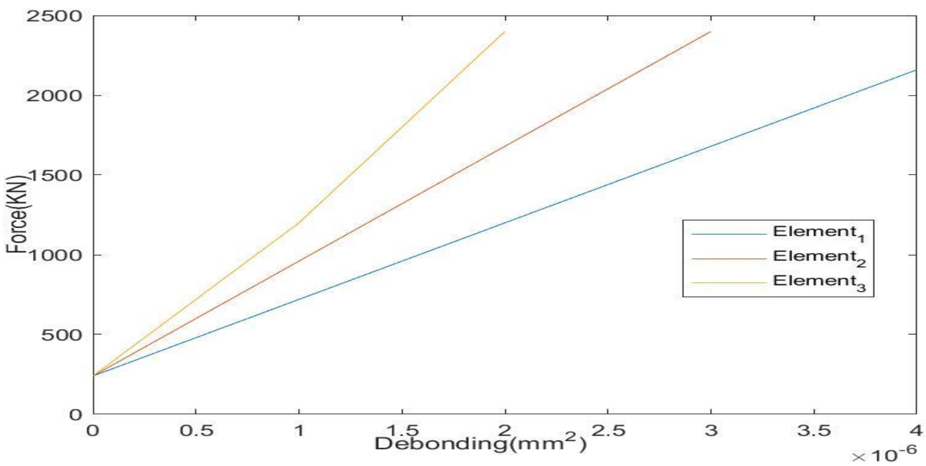

Figure 4.9: A Graphical Representation of the Force-Debonding Relationship

To know the distribution of debonding on the macrostructure, the deformation of the macrostructure was plotted by the multiscale. The deformation plot as shown in ***Figure 10***, is a result of the loading condition shown in ***Figure 4.4.***

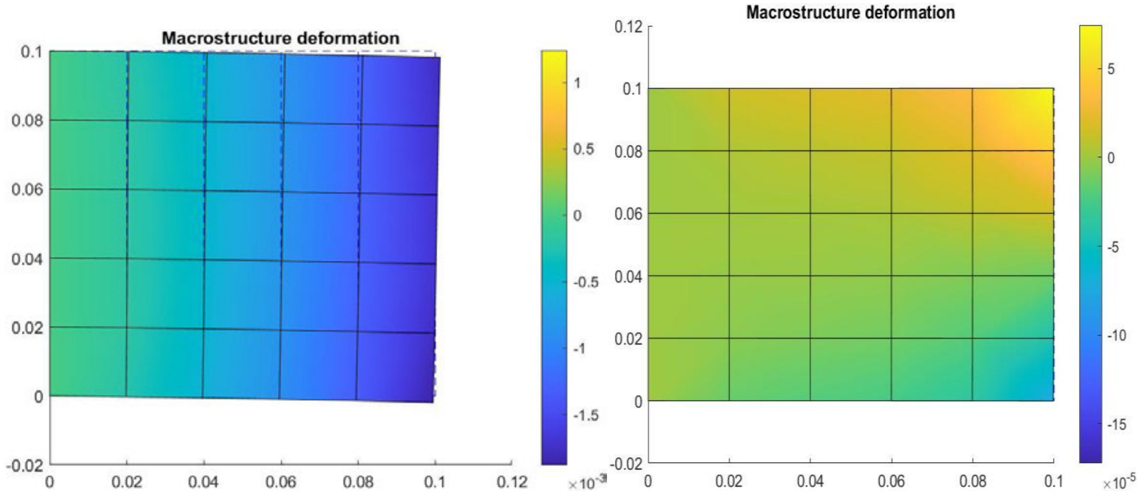

(a)**Loading Condition in Figure 4.4a** (b)**Loading Condition in Figure 4.4b**

Figure 4.10: Macrostructure Deformation

From the deformation diagram in ***Figure 4.10,*** it will be seen that there is debonding at the upper left corner of the macro model.

To check the relationship between the magnitude of applied force and debonding, the loading force in ***Figure 4.4*** was increased by a multiple of 10 units. The deformation of the macrostructure can be shown in ***Figure 4.11.***

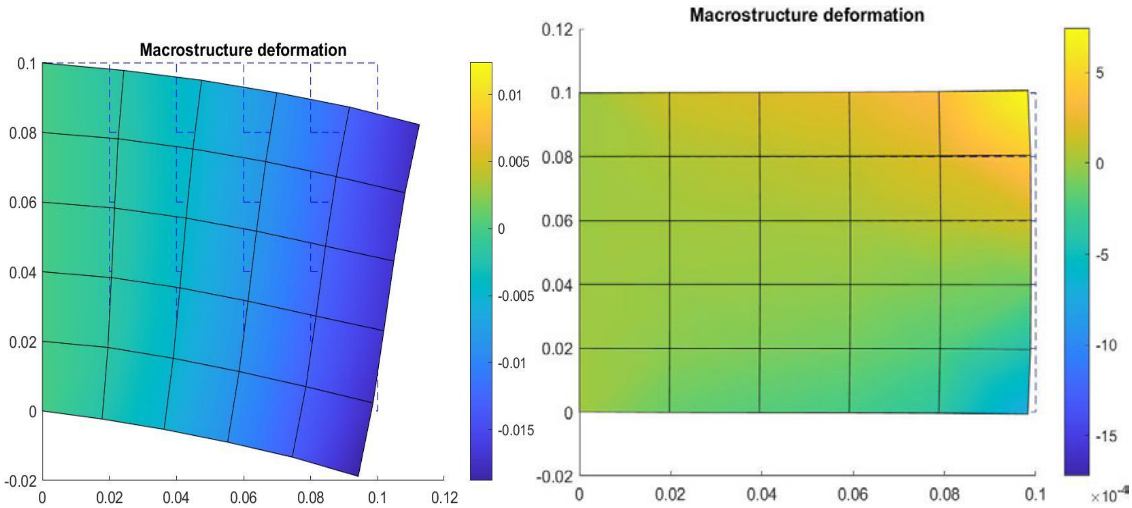

(a)**Loading Condition in Figure 4.4a** (b)**Loading Condition in Figure 4.4b**

Figure 4.11: Macrostructure Deformation Resulting from Increased Loading of multiple of 10units

From ***Figure 4.11,*** it can be seen that the structure experienced a larger deformation as a result of the increased loading by a multiple of 10units. With the above observation, it can be inferred that the increase in loading force increases the debonding between the constituents of the composites.

Effect of Change in Shape and Dimensions of the Macrostructure

To test the effect of dimensions and shape of the macrostructure, the dimension was changed from a square of size 0.1m by 0.1m to a square of 0.2m by 0.2m, it was observed that there isn't a change in the force-displacement relationship as shown in ***Figure 4.12.***

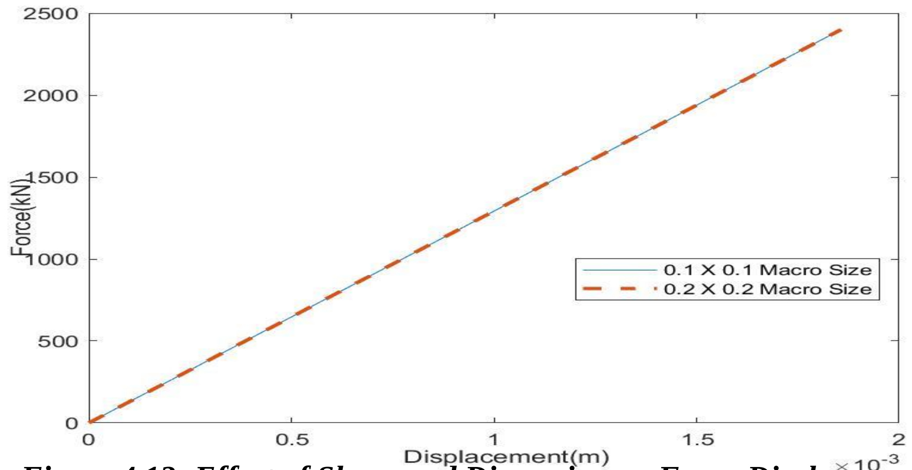

Figure 4.12: Effect of Shape and Dimension on Force-Displacement Relationship

The shape of the Macroscale was changed from a square of dimension 0.1m by 0.1m to a rectangle of dimension 0.2m X 0.1m. It was observed that there was a change in the force-displacement diagram as shown in ***Figure 4.13.***

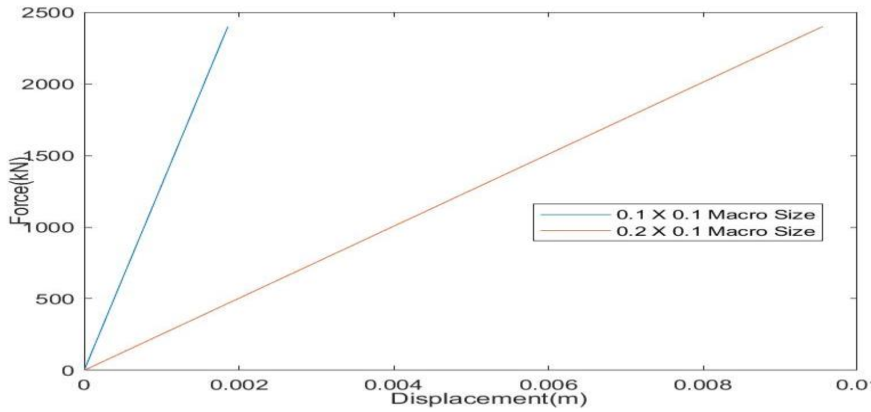

Figure 4.13: Effect of Shape on Force-Displacement Relationship

From ***Figure 4.13,*** it is seen that the macrostructure with a rectangular shape suffers more displacement if the same force is applied to both structures. The deformation of the rectangular-shaped macrostructure was also plotted and it is shown in ***Figure 4.14.***

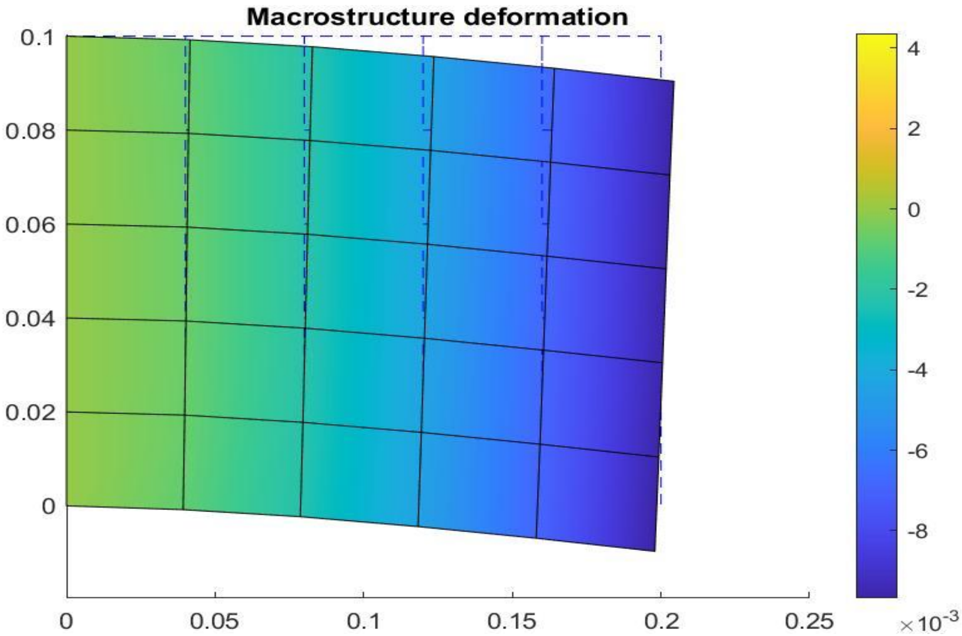

Figure 4.14: Deformation as a Result of Change in Shape of the Macrostructure

From ***Figure 4.14,*** it can be seen that the structure experienced a larger deformation than it experienced when the shape is a square. With this observation, it can be inferred that a change in the shape and dimension of the macrostructure is a factor that influences how the macrostructure of the fibre-reinforced composites deforms.

4.3 COMPARISON BETWEEN TRADITIONAL MULTISCALE COMPUTATIONAL HOMOGENIZATION AND DATA-DRIVEN MULTISCALE COMPUTATIONAL HOMOGENIZATION

In this section, the results from the traditional multiscale computational homogenization will be compared to those received from data-driven multiscale computational homogenization.

The traditional computational multiscale computational homogenization involves the simulation of the RVE first and the results from the RVE are used in solving for the effective behaviour of the macrostructure. After the simulation of the RVE, the RVE deformation is shown in ***Figure 4.15.***

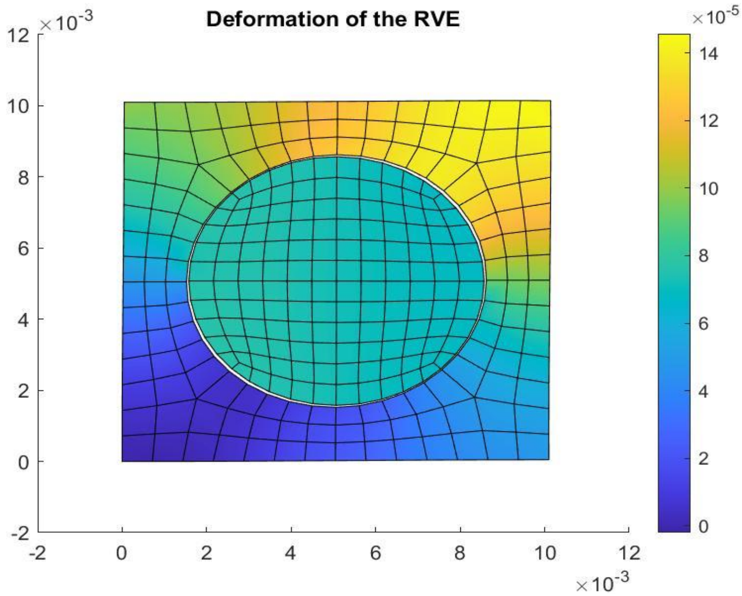

Figure 4.15: Deformation of the RVE

The diagram of the deformation of the RVE in ***Figure 4.15,*** shows that there is a displacement jump which shows that the loading strain which is used in the simulation of the RVE caused debonding between the constituents of the composite structure.

The diagram of the deformation of the RVE in ***Figure 4.15,*** is a function of a loading strain of range -0.01 to 0.01 with a loading step of 0.01. The loading step was increased from 0.01 to 0.02 and the deformation was the same as shown in ***Figure 4.16***

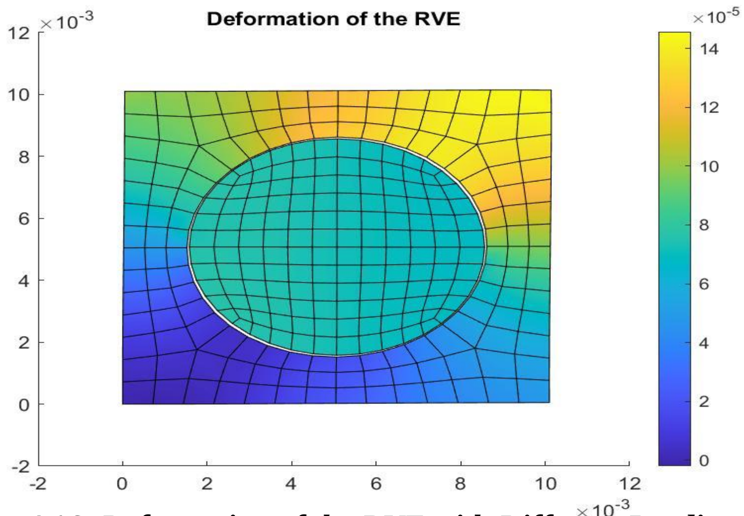

Figure 4.16: Deformation of the RVE with Different Loading Strain

To investigate the effect of loading strain on the deformation of the RVE, the loading strain of range -0.02 to 0.02 with a loading step of 0.02 and a loading strain of range -0.1 to 0.1 with a loading step of 0.02 was loaded on the structure. The result is shown in ***Figure 4.17*** and ***Figure 4.18*** respectively.

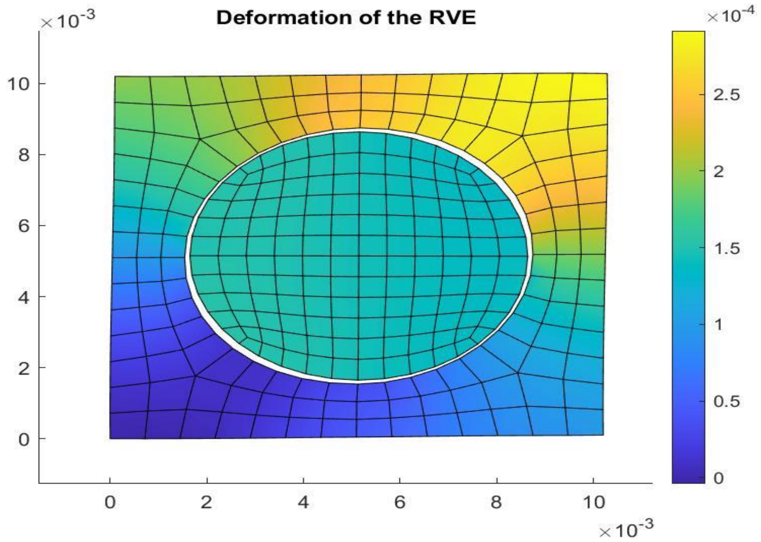

Figure 4.17: Deformation of the RVE with Different Loading Strain

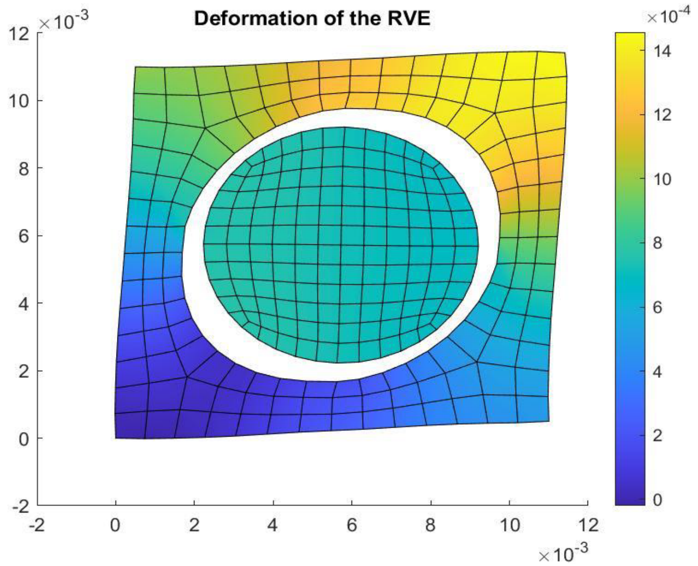

Figure 4.18: Deformation of the RVE with Different Loading Strain

Figure 4.15, Figure 4.16, Figure 4.17, and ***Figure 4.18*** show that that the displacement jump which results in debonding between the constituents of the composite is a function of the range of the loading strain and not the loading step. This is shown in the gap shown in each diagram.

In ***Figure 4.15 and Figure 4.16,*** both deformation diagram has the same loading strain range of -1 to 1, and the gap is the same even though both have different loading steps. But ***Figure 4.17*** and ***Figure 4.18,*** both have different loading strain ranges but the same loading step. This resulted in both having different gaps with ***Figure 4.18,*** having a bigger gap as a result of a bigger strain range.

With these observations, it can be inferred that the more the loading strain range, the bigger the displacement jump and debonding. The strain range of -1 to 1 with a loading step of 0.1 was used for this research.

The results from the simulation of the RVE were incorporated in a Multi-scale Macro-Increment MATLAB Code and the loading in ***Figure 4.4(a)*** is used as a model for the macrostructure. After simulation, the result for the force-displacement relationship and macrostructural deformation is shown in ***Figures 19 (a)*** and ***(b)*** respectively**.**

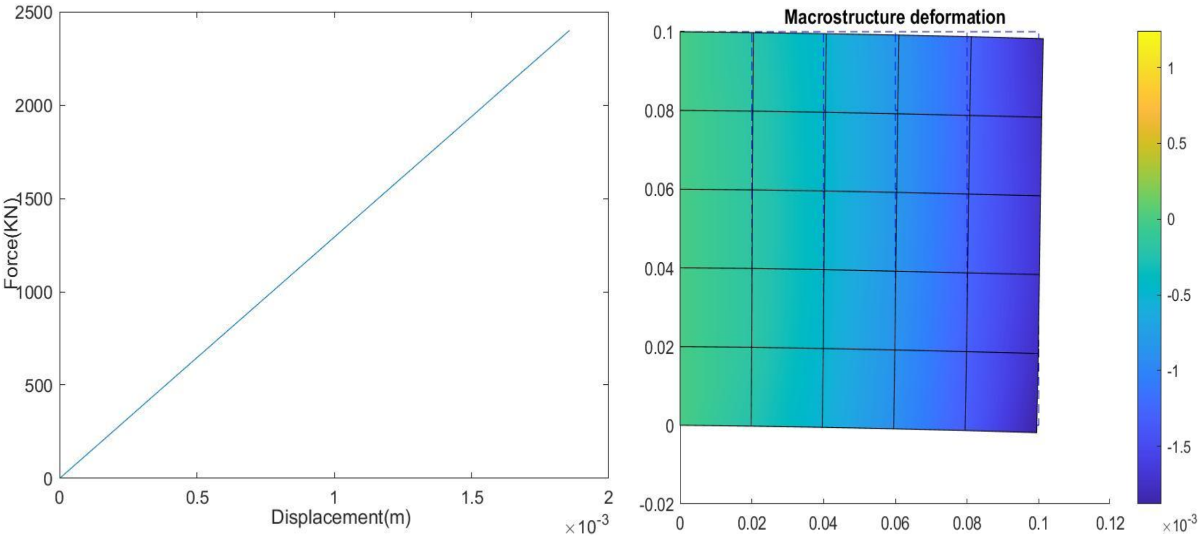

Figure 4.19: (a)Force Displacement Graph (b) Macrostructure Deformation

From ***Figure 4.19(a),*** it can be inferred that an increase in force leads to an increment in the displacement of the structure. This resulted in a linear graph with a positive slope.

Figure 4.19(b), shows that there was debonding in the constituents located in the upper left corner of the composite.

The force-displacement relationship of the traditional multi-scale homogenization as a result of the loading condition shown in ***Figure 4.4(a)*** was compared to that of the data-driven multiscale homogenization. The result of the comparison is shown in ***Figure 4.20.***

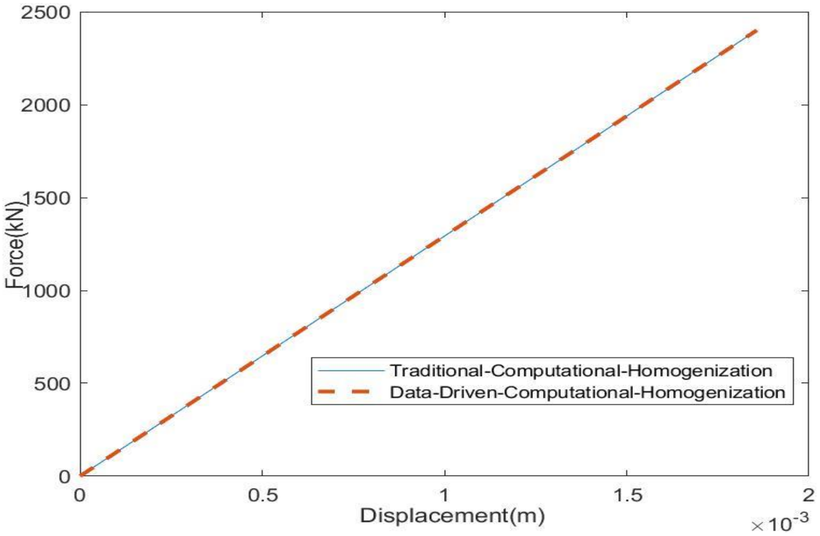

Figure 4.20: Comparison between Traditional and Data-Driven Multiscale Computation

From the comparison in ***Figure 4.20,*** it can be seen that the relationship between the applied force and displacement for both methods is the same. This shows that both methods give the same result.

Furthermore, the loading condition shown in ***Figure 4.7*** was also adopted. This resulted in a non-linear relationship in the force-displacement graph as shown in ***Figure 4.18.***

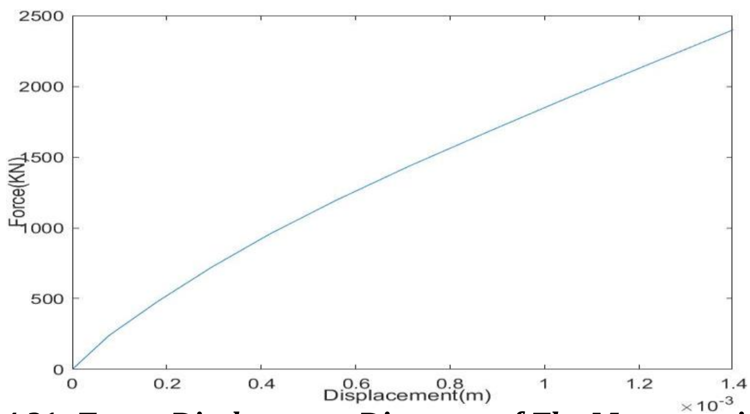

Figure 4.21: Force–Displacement Diagrams of The Macroscopic Structure for a Combined Loading

The non-linear relationship that is shown in ***Figure 4.21,*** shows the change in the orientation of the contact state in the interface of the composite structure.

Again, the force-displacement relationship of the traditional multi-scale homogenization as a result of the loading condition shown in ***Figure 4.7*** was compared to that of the data-driven multiscale homogenization. The result of the comparison is shown in ***Figure 4.22.***

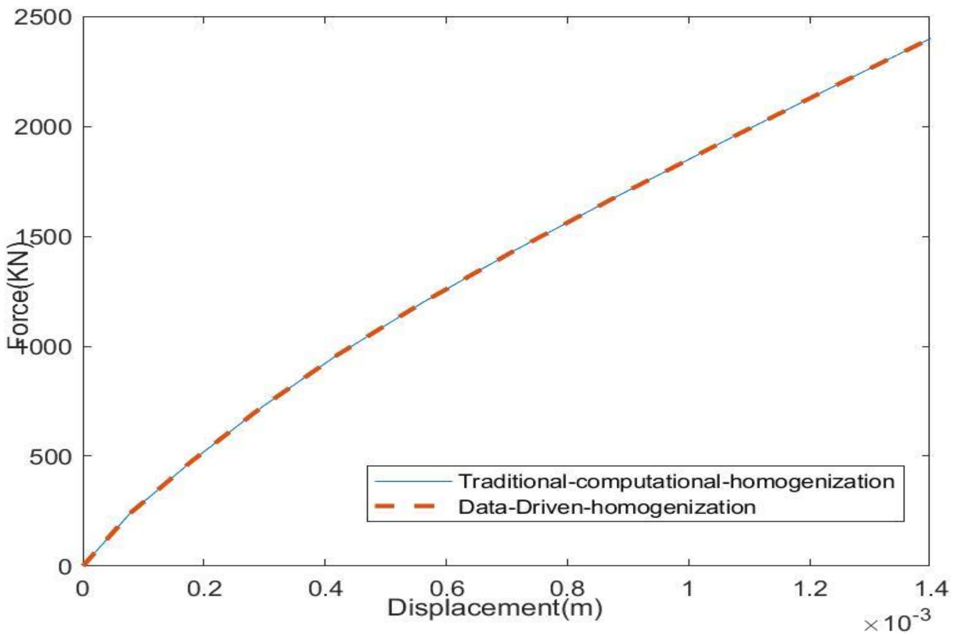

Figure 4.22: Comparison between Traditional and Data-Driven Multiscale Computation

From the comparison in ***Figure 4.22,*** it can be seen that the relationship between the applied force and displacement for both methods is the same. The nonlinear relationship shows that there is a change in the contact state in the interface between the fibre and matrix.

To investigate the effect of the magnitude of applied load on the deformation of the macrostructure when using the traditional multiscale computational homogenization, the load on the macrostructure is increased by a multiple of 10units. The deformation of the macrostructure as a result of the applied new load is given in ***Figure 4.23.***

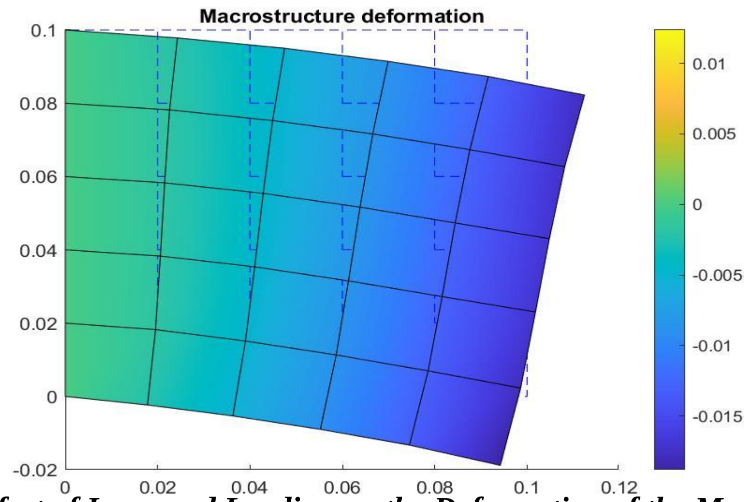

Figure 4.23: Effect of Increased Loading on the Deformation of the Macrostructure

From ***Figure 4.11,*** it can be seen that the structure experienced a larger deformation as a result of the increased loading by a multiple of 10units. With the above observation, it can be inferred that the increase in loading force increases the debonding between the constituents of the composites.

Also, to investigate the effect of dimension and shape on the deformation of the macrostructure when using the traditional multiscale computational homogenization, the shape of the macrostructure is changed from a square of side 0.1m to a rectangle of size 0.2m by 0.1m while retaining the original load. The deformation of the macrostructure as a result of the new shape is given in ***Figure 4.24.***

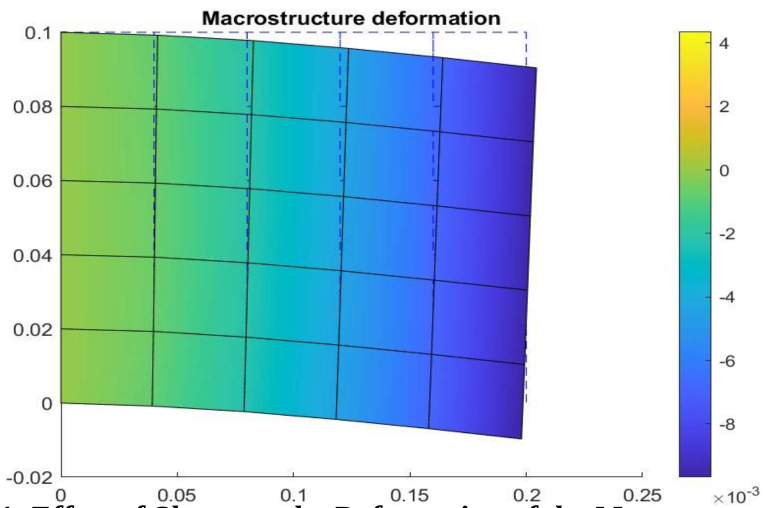

Figure 4.24: Effect of Shape on the Deformation of the Macrostructure

From ***Figure 4.24,*** it can be seen that the structure experienced a larger deformation than it experienced when the shape is a square. With this observation, it can be inferred that a change in the shape and dimension of the macrostructure is a factor that influences how the macrostructure of the fibre-reinforced composites deforms.

CONCLUSION

In this research, a multi-scale finite element method that makes use of a database and Artificial Neural Network has been adopted. This method is a combination of the computational finite element method and sophisticated data-driven metamodels.

Representative Volume Element (RVE) was first simulated, and the simulation gave the RVE deformation which was shown in ***Figure4.15.*** The diagram showed that there was a displacement jump after the RVE simulation which lead to debonding between the constituents that made up the composite. Debonding occurs in a composite material when there is a separation in the interface between the constituents that make up the composite.

The deformation of the RVE is a function of the loading strain range and not necessarily the loading step. This is shown in ***Figure 4.15*** and ***Figure 4.16,*** which gave the same RVE deformation diagram, and ***Figure 4.17*** and ***Figure 4.18,*** which gave different results. For this research, the loading strain range of -1 to 1 with the loading step of 0.1 was used since it generated more results used as the database for the data-driven multiscale homogenization.

The results calculated using the RVE were incorporated in Multi-scale Macro-Increment MATLAB Code to simulate the macrostructure using traditional multiscale computational homogenization to get the effective properties of the composite.

The microscopic stress and stiffness gotten from the finite element simulation of the RVE are what formed the database used for data-driven computational homogenization which is the major methodology used in this research.

From the macrostructural deformation, diagrams are shown in this research it can be seen the rate of deformation is influenced by the magnitude and direction of the force. Also, the deformation is a function of the shape of the macrostructure.

In the simulations of the RVE, the properties of the macrostructure depend on the contact state at the interface of the constituents of the composite. The contact state is affected by the loading strain and also affected by the nature and magnitude of load applied to the macrostructure, which in turn affects the properties and behaviour of the macrostructure. This change in contact state as a result of applied load can be seen in the change in the force-displacement graph, from linear to non-linear. Debonding reduces the stiffness of the composite and is caused by the nature of force applied at the macroscale.

From the comparison between traditional multiscale computational homogenization and data-driven multiscale computation homogenization as ***shown*** in ***Figure 4.17*** and ***Figure 4.19,*** it can be inferred that both methods gave a good and the same result but the data-driven method advantages because it is more straightforward and the computational time is less expensive when compared to the traditional multiscale computational homogenization method

Furthermore, the accuracy of data-driven multiscale homogenization depends on the accuracy of the NN training. Even though ANN gives an accurate result, more sophisticated packages like Convolution Neural Network (CNN) and Deep Learning will give a more accurate result. Also, the use of data-driven can be extended to the use of data from the experimental database. This will be very important in the analysis of complex composites whose properties have been monitored experimentally.

Data-driven computational homogenization can also find its usefulness in other areas of structural engineering such as the Extended Finite Element Method (X-FEM) and Physics Informed Neural Networks (PINNs). X-FEM is an enhanced FEM that is suitable for crack-propagation simulation because it solves discontinuity in functions which is not easy using conventional FEM. PINNs are deep-learning networks that, given an input point in the integration domain, produce an approximated solution of a differential equation/equation after training (solving an optimization problem to minimize a residual function) (called collocation point). These two areas are areas of future research.

REFERENCES

Aldakheel, F., Satari, R., & Wriggers, P. (2021). Feed-Forward Neural Networks for Failure Mechanics Problems. (C. M. A., Ed.) *Applied Sciences*. doi:https://doi.org/10.3390/app11146483

Andreassen, E., & Andreasen, C. S. (2014). How to determine composite material properties using numerical homogenization. *Computational Materials Science, 83*, 488-495. doi:10.1016/j.commatsci.2013.09.006

ANITS. (2020). *ANITS*. Retrieved October 11, 2021, from https://www.anits.edu.in/online_tutorials/UNIT%205.pdf

Antoine, G. (2012, September). Numerical homogenization: survey, new results, and perspectives. (E. Canc`es and S. Labb´e, Ed.) *ESAIM: Proceedings,, 37*, 50-116. doi:10.1051/proc/201237002

Arbabi, H., Bunder , J. E., Samaey, G., Roberts, A. J., & Kervrekidis, I. G. (2020). Linking Machine Learning with Multiscale Numerics:. *The Minerals, Metals & Materials Society*, 1-14.

Atsuya Oishia, & Genki Yagawa. (2017). Computational mechanics enhanced by deep learning. *Comput. Methods Appl. Mech. En*, 327–351.

Avery, P., Huang, D. Z., He, W., Ehlers, J., & Derkevorkian, A. (2021). A Computationally Tractable Framework for Nonlinear Dynamic Multiscale Modelling of MembraneWoven Fabrics. *Int. J. Numer. Methods Eng., 122*, 2598–2625. doi: 10.1002/nme.6634

Bacigalupo, A., & Gambarotta, L. (2010). Second-order computational homogenization of heterogeneous materials with periodic microstructure. *ZAMM · Z. Angew. Math. Mech, 90*(10 – 11), 796 – 811. doi:10.1002/zamm.201000031

Bahl, S. (2021). Fibre reinforced metal matrix composites - a review. *Materials Today: Proceedings, 39*, 317–323. doi:https://doi.org/10.1016/j.matpr.2020.07.423

Balokas, G., Czichon, S., & Rolfes, R. (2018). Neural network assisted multiscale analysis for the elastic properties prediction of 3D braided composites under uncertainty. *Composite Structures, 183*, 550–562. doi:http://dx.doi.org/10.1016/j.compstruct.2017.06.037

Barberto, E. J. (2011). *Introduction to Composite Materials design.* New York: Taylor & Francis Group.

Beluch, W., & Hatlas, M. (2018, January 08). Numerical Homogenization of Inhomogeneous Media with Imprecise Parameters. *Computer Methods in Mechanics, 1922*, 030006-1–030006-7;. doi:10.1063/1.5019040

Bensoussan, A., Lions, J.-L., & Papanicolaou, G. (1978). Asymptotic Analysis for Periodic Structures. (L. J.L., G. Papanicolaou, & R. Rockafellar, Eds.) *Studies in Mathematics and its Applications, 5*, 721. Retrieved October 13, 2021

Benveniste, Y., & Aboudi, J. (1984). A Continuum Model for Fibre Reinforced Materials with Debonding. *Int. J. Solids Structures, 20*, 935-951. Retrieved October 03, 2021

Blessley, D. (n.d.). *Academia*. Retrieved October 10, 2021, from https://www.academia.edu/7487930/Module_1_General_Introduction_M1_General_Introduction

Bunsell, A. R. (2001). Fibres with High Modulus. *Encyclopadia of Materials: Science and Technology (Second Edition)*, 3151-3157.

Campbell, F. (2010). Introduction to Composite Materials. In *Structural Composite Materials* (pp. 1-30). ASM International.

Car, E., Oller, S., & Oñate, E. (2000). An anisotropic elastoplastic constitutive model for large strain analysis of ®ber reinforced composite materials. *Comput. Methods Appl. Mech. Engrg, 185*, 245-277.

Car, E., Zalamea, F., Oller, S., Miquel, J., & Onate, E. (2002). Numerical simulation of fibre reinforced. *International Journal of Solids and Structures, 39*, 1967–1986.

Chen, Y., & Schuh, C. A. (2009, March 10). Analytical homogenization method for periodic composite materials. *Physical Review B, 79*, 094104-094113. doi:10.1103/PhysRevB.79.094104

Conti, S., Müller, S., & Ortiz, M. (2018). Data-Driven Problems in Elasticity. *Arch. Rational Mech. Anal.*, 1-45. doi:10.1007/s00205-017-1214-0

Dascalu, C., Bilbie, G., & Agiasofitou, E. (2008). Damage and size effects in elastic solids:A homogenization approach. *International Journal of Solids and Structures 4, 45*, 409-430. doi:10.1016/j.ijsolstr.2007.08.025

Datoo, M. H. (1991). *Mechanics of Fibrous Composite* (1st ed.). New York, USA: Elsivier Science Publishing LTD.

Dhakal, H. N., & Ismail, S. O. (2021). *Sustainable Composites for Lightweight Applications.* United Kingdom: Matthew Deans.

Drosopoulos, G. A., & Stavroulakis, G. E. (2020). Data-driven Computational Homogenization Using Neural Networks:FE2-NN Application on Damaged Masonry. *ACM Journal on Computing and Cultural Heritage,*, 19.

Drosopoulos, G. A., Giannis, K., Stavroulaki, M. E., & Stavroulakis, G. E. (2018). Metamodelling Assisted-Numerical Homogenation for Masonry and Cracked Structures. *Journal of Engineering Mechanics*, 35. doi:10.1061/(ASCE)EM.1943-7889.0001500

Drosopoulos, G. A., Wriggers, P., & Stavroulakis, G. E. (2014). A multi-scale computational method including contact for the analysis of damage in composite materials. *Computational Materials Science, 95*, 522-535. doi:10.1016/j.commatsci.2014.08.004

Drosopoulos, G. A., Wriggers, P., & Stavroulakis, G. E. (2014). A multi-scale computational method including contact for the analysisof damage in composite materials. *Computational Materials Science*, 522–535.

Drugan, W. J., & Willis, J. R. (1996). A Microscopic-Based Nonlocal Constitutive Equation and Estimates of Respresentative Volume Element Size For Elastic Composites. *J. Mech. Phys. Solids,, 44*(4), 497-524.

Efendiev, Y., & Hou, T. Y. (2009). *Multiscale Finite Element Methods: Theory and application.* USA: Springer-Verlag New York.

Efendiev, Y., & Pankov, A. (2004). Numerical Homogenization and Correctors for Nonlinear Elliptic Equations. *SIAM Journal on Applied Mathematics, 65*, 43-68. Retrieved October 14, 2021, from https://www.jstor.org/stable/4096213

Escoda, J., Willot, F., Jeulin, D., Sanahuja, J., & Toulemonde, C. (2011). Estimation of local stresses and elastic properties of a mortar sample by FFT computation of fields on a 3D image. *Cement and Concrete Research, V*(41), 542-556.

Fish, J., & Yu, Q. (2001). Multiscale damage modelling for composite materials: theory and computational framework. *International journal for numerical methods in Engineering, 52*, 161–191. doi:10.1002/nme.276

Garmestani, H. (1997). *Mechanical and Microscopy Analysis of Carbon Fibre Reinforced Polymetric Matrix Composite Material.* Florida: Florida Department of Transportation.

Geers, M. G., Coenen, E. W., & Kouznetsova, V. G. (2007). Multi-scale computational homogenization of structured thin sheets. *Modelling Simul. Mater. Sci. Eng., 15*, 393 - 404. doi:10.1088/0965-0393/15/4/S06

Geers, M. G., Kouznetsova, V. G., & Brekelmans, W. A. (2010). Multi-scale computational homogenization: Trends and challenges. *Journal of Computational and Applied Mathematics, 234*, 2175-2182. doi:10.1016/j.cam.2009.08.077

Geers, M. G., Kouznetsova, V. G., Matouš, K., & Yvonnet, J. (2017). Homogenization Methods and Multiscale Modelling: Nonlinear Problems. (R. d. Erwin Stein, Ed.) *Encyclopedia of Computational Mechanics Second Edition*, 34. doi:10.1002/9781119176817.ecm2107

Georgiadis, S. A., Stavroulak, G. E., Koltsakis, E. K., & Panagiotopoulos, P. D. (1990). Interfacial Debonding In Composites Via Mathematical Programming Methods; The Material Inclusion Problem for Lubricated and Non-Lubricated Interfaces. *computers& strucrures, 34*, 735-752. Retrieved October 1, 2021

Goda, T., Váradi, K., & Friedrich, K. (2001). Fe micro-models to study contact states, stresses and failure mechanisms in a polymer composite subjected to a sliding steel asperity. *Wear*(251), 1584–1590.

Green, A. E., & Naghdi, P. M. (1965). A Dynamical Theory of Interacting Continua. *Inf. J. Engng Sci., III*, 231-241.

Guede, J., & Kikuchi, N. (1990). Preprocessing and postprocessing for materials based on the homogenization method with adaptive finite element methods. *Computer Methods in Applied Mechanics and Engineering, 83*(2), 143-198.

Henkes, A., Caylak, I., & Mahnken, R. (2021). A deep learning driven pseudospectral PCE based FFT homogenization algorithm for complex microstructures. *Comput. Methods Appl. Mech. Engrg, 385*, 114070 - 114096.

Herakovich, C. T. (1998). *Mechanics of Fibrous Composites* (1st ed.). New York: John Wiley & Sons, Inc.

Herakovich, C. T. (1998). *Mechanics of Fibrous Composites.* New York: John Wiley & Sons, Inc.

Hill, R. (1963, April 4). Elastic Properties of Reinforced Solids: Some Theoretical Principles. *J. Mech. Phys. Solids, I I*, 357 - 372. Retrieved September 27, 2021

Hirschberger, B. C., Ricker, S., Steinmann, P., & Sukumar, N. (2009). Computational multiscale modelling of heterogeneous material layers. *Engineering Fracture Mechanics, 76*, 793–812. doi:10.1016/j.engfracmech.2008.10.018

Hui, D., & Dutta, P. (1998). Use of Composites in Infrastructure. *Advanced Multilayered and Fibre-Reinforced Composites, 43*, 3-11.

Hutton, D. V. (2004). *Fundamentals of Finite Element Analysis* (1st ed.). New York: The McGraw-Hill Companies, Inc.,.

Jagota, V., Sethi, A. S., & Kumar, K. (2013). Finite Element Method: An Overview. *Walailak J Sci & Tech*, 1-8.

Kaczmarczyk, Ł., Pearce, C. J., & Bic´anic´, N. (2010). Studies of microstructural size effect and higher-order deformation in second-order computational homogenization. *Computers and Structures, 88*, 1383–1390. doi:10.1016/j.compstruc.2008.08.004

Kalamkarov, A. L., Andrianov, I. V., & Danishevs'kyy, V. V. (2009, May). Asymptotic Homogenization of Composite Materials and Structures. *Applied Mechanics Reviews, 62*, 030802-03101. doi:10.1115/1.3090830

Karapiperis, K., Stainier, L., Ortiz, M., & Andrade, J. (2021). Data-Driven multiscale modelling in mechanics. *J. Mech. Phys. Solids, 147*, 104239-104255.

Kirchdoerfer, T., & Ortiz, M. (2016). Data-driven computational mechanics. *Comput. Methods Appl. Mech. Engrg*, 81-101.

Korzeniowski, T. F., & Weinberg, K. (2021). A multi-level method for data-driven finite element computations. *Comput. Methods Appl. Mech. Engrg*, 13.

Kouznetsova, V. G. (2002). *Computational homogenization for the multi-scale analysis of multi-phase Material.* Retrieved from ttps://doi.org/10.6100/IR560009

Kouznetsova, V., Geers, M., & Brekelmans, W. (2002). Multi-scale constitutive modelling of heterogeneous materials with a gradient-enhanced computational homogenization scheme. *Int. J. Numer. Meth. Engng, 54*, 1235–1260. doi:10.1002/nme.541)

Kouznetsova, V., Geers, M., & Brekelmans, W. (2004). Multi-scale second-order computational homogenization of multi-phase materials: a nested finite element solution strategy. *Comput. Methods Appl. Mech. Engrg., 193*, 5525–5550. doi:10.1016/j.cma.2003.12.073

Krushynska, A., Kouznetsova, V., & Geers, M. (2014). Towards optimal design of locally resonantacoustic metamaterials. *Journal of the Mechanics and Physics of Solids*(71), 179-196.

Le, B. D., Dau, F., Pham, D. H., & Tran, T. D. (2021). Discrete element modelling of interface debonding behaviour in compositematerial: Application to a fragmentation test. *Composite Structures, 272*, 114170-114178. doi:10.1016/j.compstruct.2021.114170

Lectures, F. (n.d.). *Engineering and Computer Science University of Victoria.* Retrieved 08 25, 2021, from google: https://www.engr.uvic.ca/~mech410/lectures/FEA_Theory.pdf

Lenglet, E., Hladky-Hennion, A.-C., & Debus, J.-C. (2003). Numerical homogenization techniques applied to piezoelectric composites. *J. Acoust. Soc. Am., 113*, 1-8. doi:10.1121/1.1537710#

Li, E., Zhang, Z., Chang, C. C., Liu, G. R., & Li, Q. (2015). Numerical homogenization for incompressible materials using selective smoothed finite element method. *Composite Structures, 123*, 216–232. doi:10.1016/j.compstruct.2014.12.016

Linero, D. L., Oliver, J., & Huespe, A. (2007). *A model of material failure for reinforced concrete via continuum bstrong discontinuity approach and mixing theory* (Primera edición ed.). Barcelona, Spain: Los autores.

Liu, X., Tain, S., Tao, F., & Yu, W. (2021). A review of artificial neural networks in the constitutive modelling of composite materials. *Composites Part B*, 15. Retrieved from www.elsevier.com/locate/composites

Lu, X., Giovanis, D. G., Yvonnet, J., Papadopoulos, V., Detrez, F., & Bai, J. (2018, September 22). A data-driven computational homogenization method based on neural networks for the nonlinear anisotropic electrical response of graphene/polymer nanocomposites. *Computational Mechanics*, 15. Retrieved from https://doi.org/10.1007/s00466-018-1643-0

Lu, X., Yvonnet, J., Papadopoulos, L., Kalogeris, I., & Papadopoulos, V. (2021). A Stochastic FE2 Data-Driven Method for Nonlinear. *Materials, 14*, 2875-2897. doi:10.3390/ma14112875

Marti'nez, X. (2008). *Micro Mechanical Simulation of Composite Materials Using the Serial /Parallel Mixing Theory.* Barcelona: Doctoral Theisis.

Martinez, X., Oller, S., Rastellini, F., & Barbat, A. H. (2008). A numerical procedure simulating RC structures reinforced with FRP using the serial/parallel mixing theory. *Computers and Structures, 86*, 1604–1618.

Michel, J., Moulinee, H., & Suquet, P. (1999). Effective properties of composite materials with periodic microstructure: a computational approach. *Comput. Methods Appl. Mech. Engrg, 172*, 109-143. Retrieved October 14, 2021

Miehe, C., & Koch, A. (2002). Computational micro-to-macro transitions of discretized microstructures undergoing small strains. *Archive of Applied Mechanics, 72*, 300 – 317. doi:10.1007/s00419-002-0212-2

Montáns, F. J., Chinesta, F., Gómez-Bombarelli, R., & Kutz, J. N. (2019). Data-driven modelling and learning in science and engineering. *Comptes Rendus Mecanique, 347*, 845–855. doi:10.1016/j.crme.2019.11.009

Nemat-Nasser, S., & Hori, M. (1993). *Micromechanics: Overall properties of Heterogeneous Material.* Amsterdam, Netherland: Elsevier Science Publishers.

Nguyen, V. P., Stroeven, M., & Sluys, L. J. (2011). Multiscale Continous and Discountinous Modelling of Heterogeneous Materials: A Review on Recent Development. *Journal of Multiscale Modelling, III*(4), 229-270. doi:10.1142/S1756973711000509

Nikishkov, G. P. (2004). *Introduction to the Finite Element Method .* Japan.

Okereke, M., & Keates, S. (2018). *Finite Element Applications; A Practical Guide to the FEM Process* (1st ed.). Gewerbestrasse, Cham,, Switzerland: Springer International Publishing. doi:10.1007/978-3-319-67125-3

Oller, S. (2014). *Numerical Simulation of Mechanical Behaviour of Composite Materials* (1st ed.). Barcelona, Spain: International Center for Numerical Methods in Engineering.

Oller, S. (2014). *Numerical Simulation of Mechanical Behaviour of Composite Materials* (1st ed.). (O. Eugenio, Ed.) Barcelona, Spain: Springer.

Oller, S., Oñate, E., Miquel, J., & Botello, S. (1996). A Plastic Damage Constitutive Model for Composite Material. *Im. J. Solids Structures, 33*, 2501-2518.

Ortiz, M., & PoPov, E. P. (1982). A physical model for the inelasticity of concrete. *Proceedings of the Royal Society of London, 383*(1784), 101-125. Retrieved from http://www.jstor.org/stable/2397353

Ortiz, M., & Popov, E. P. (1982). Plain Concrete asa composite Material. *Mechanics of Materials, 1*, 139-150.

Otero, F., Oller, S., Martinez, X., & Salomón, O. (2015). Numerical homogenization for composite materials analysis; Comparison with other micro mechanical formulations. *Composite Structures, 122*, 405–416. doi:http://dx.doi.org/10.1016/j.compstruct.2014.11.041

Ouchetto, O., Qiu, C.-W., Zouhdi,, S., Li, L.-W., & Razek, A. (2006, November). Homogenization of 3-D Periodic Bianisotropic Metamaterials. *IEEE Transactions on Microwave Theory and Techniques, LIV*(11), 3893-3898. doi:10.1109/TMTT.2006.885082

Paggi, M., Carpinteri, A., & Zavarise, G. (1949). A unified interface constitutive law for the study of fracture and contact problems in heterogeneous materials. *ASME J. Appl.Mech., 16*, 259-268.

Patel, B., & Zohdi, T. I. (2016). Numerical estimation of effective electromagnetic properties for design. *Materials and Design*(94), 546–553.

Sanchez-Palencia, E. (1980). *Non-Homogeneous Media and Vibration Theory* (Vol. 127). (M. K. J. Ehlers, Ed.) New York: Springer-Verlag New York Heidelberg Berlin. Retrieved October 13, 2021

Schröder, J., Labusch, M., & Keip, M.-A. (2016). Algorithmic two-scale transition for magneto-electro-mechanically coupled problems. *Computer Methods in Applied Mechanics and Engineering* (302), 253-280.

Seshu, P. (2003). *Textbook of Finite Element Analysis* (10th ed.). New Delhi: PHI Private Limited.

Shu, W., & Stanciulescu, I. (2020). Multiscale homogenization method for the prediction of elastic properties of fibre-reinforced composites. *International Journal of Solids and Structures, 203*, 249–263.

Siddiq, M. (2020). Data-driven finite element method:Theory and applications. *J Mechanical Engineering Science, 0*, 1-11. doi:10.1177/0954406220938805

Skansi, S. (2018). *Introduction to Deep Learning.* Zagreb, Zagreb, Croatia: Springer International Publishing AG,. Retrieved August 25, 2021, from https://doi.org/10.1007/978-3-319-73004-2

Stavroulakis, G., Avdelas, A., Abdalla, K., & Panagiotopoulos, P. (1997). A Neural Network Approach to the Modelling, Calculation and Identification of Semi-Rigid Connections in Steel Structures. *J. Construct. Steel Res., 44*(1-2), 91-105.

Suquet, P. M. (1985). Local and Global Aspects in the Mathematical Theory of Plasticity. In A. Sawczuk, & G. Bianchi (Eds.), *Plasticity today; Modelling, Methods and Application* (pp. 279-310). London and New York: Elsivier Applied Science Publishers.

Terada, K., & Kikuchi, N. (2001). A class of general algorithms for multi-scale analyses of heterogeneous media. *Comput. Methods Appl. Mech. Engrg., 190*, 5427-5464.

Terada, K., Hori, M., Takashi, K., & Kikuchi, N. (2000). Simulation of the multi-scale convergence in computational homogenization approaches. *International Journal of Solids and Structures*, 2285±2311.

Tikarrouchine, E., Benaarbia, A., Chatzigeorgiou, G., & Meraghni, F. (2021). Non-linear FE2 multiscale simulation of damage, micro and macroscopic strains in polyamide 66-woven composite structures: Analysis and experimental validation. *Composite Structures*, 112926 - 112945.

Trusdell, C., & Toupin, R. (1960). The Classical Field Theories. *Handbuch der Physik III/I,*.

Unger, J. F., & Könke, C. (2008). Coupling of scales in a multiscale simulation using neural networks. *Computers and Structures, 86*, 1994–2003. doi:10.1016

Vasiliev, V. V., & Morozov, E. V. (2001). *Mechanics and Analysis of Composite Materials* (1st ed.). Oxford, UK, London: Elsevier Science Ltd. Retrieved 10 06, 2021

Vasiliev, V. V., & Morozov, E. V. (2001). *Mechanics and Analysis of Composite Materials* (1st Edition ed.). Oxford(UK): Elsivier Science Ltd.

Verhaegh, B. J. (2020, October 30). *Data-driven homogenization of heterogeneous micro-structures using neural networks.* Retrieved August 25, 2021, from google: https://pure.tue.nl/ws/portalfiles/portal/165891697/0810404_Verhaegh.pdf

Violeau, D., Ladevèze, P., & Lubineau, G. (2009). Micromodel-based simulations for laminated composites. *Composites Science and Technology*(69), 1364–1371.

Voyiadjis, G., & Kattan, P. (2005). *Introduction to Homogenization of Composite Materials. In: Mechanics of Composite Materials with MATLAB.* (1st ed.). Berin: Springer, Berlin, Heidelberg. doi:https://doi.org/10.1007/3-540-27710-2

Warnet, L., & Akkerman, R. (2009). Composites Course. Constituents and manufacturing techniques.

Waseem, A., Heuzé, T., Geers, M. G., Kouznetsova, V. G., & Stainiera, L. (2021). Data-driven reduced homogenization for transient diffusion problems with emergent history effects. *Comput. Methods Appl. Mech. Engrg., 380*, 113773 - 113800.

Wilson, B. (2012, November 4). *The Machine Learning Dictionary.* Retrieved November 2021, 2021, from http://www.cse.unsw.edu.au/~billw/mldict.html

Wriggers, P. (2006). *Computational Contact Mechanics* (2nd ed.). Berlin , Heidelberg, New York: Springer-Verlag. Retrieved October 3, 2021

Wriggers, P., Zavarise, G., & Zohdi, T. I. (1998). A computational study of interfacial debonding damage in fibrous composite materials. *Computational Materials Science, 12*, 39-56. Retrieved 08 21, 2021

Xiao, S., Deierling, P., Attarian, S., & El Tuhami, A. (2021). Machine learning in multiscale modelling of spatially tailored materials with microstructure uncertainties. *Computers and Structures, 249*(106511), 15. doi:https://doi.org/10.1016/j.compstruc.2021.106511

Xu, R., Yang, J., Yan, W., Huang, Q., Giunta, G., Belouettar, S., . . . Hu, H. (2020). Data-driven multiscale finite element method: From concurrence to separation. *Comput. Methods Appl. Mech. Engrg*, 112893-112907.

Yvonnet, J. (2019). *Computational Homogenization of Heterogeneous Materials with Finite Element* (Vol. 258). Switzerland: Springer Nature. doi:10.1007/978-3-030-18383-7

Zhang, L. (2015). The application of composite fibre materials in sports equipment. Wuhan, China: Published by Atlantis Press.

Zhang, X., & Garikipati, K. (2020). Machine learning materials physics: Multi-resolution neural networks learn the free energy and nonlinear elastic response of evolving microstructures. *Comput. Methods Appl. Mech. Engrg., 372*, 113362-113386.

Zimmerlinga, C., Dörr, D., Henning,, F., & Kärger, L. (2019). A machine learning assisted approach for textile formability assessment and design improvement of composite components. *Composites / A*, 1-11. doi:10.5445/IR/1000095835

Zohdi, T. I., & Wriggers, P. (2005). *Applied and Computational Mechanics; An Introduction to Computational Micromechanics* (Vol. 20). (F. Pfeiffer, & P. Wriggers, Eds.) Berlin Heidelberg, Germany: Springer-Verlag Berlin Heidelberg. Retrieved May 03, 2021